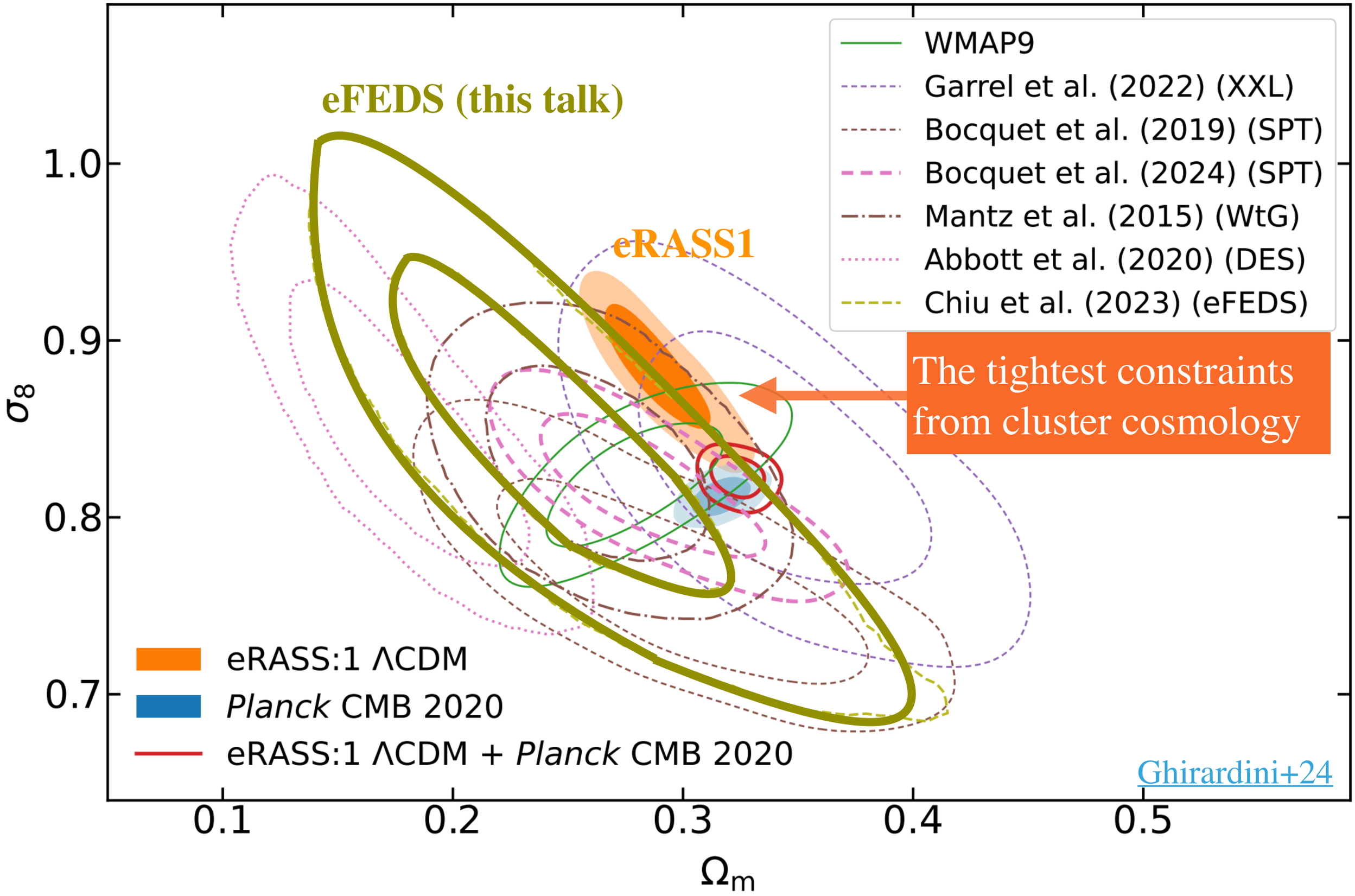
Cluster Cosmology From the eROSITA Final Equatorial Depth Survey (eFEDS)— *First Cosmological Constraints From eROSITA Clusters*

I-Non Chiu (National Cheng Kung University)

Grandis+20 (2020MNRAS.498..771G): Empirical modelling of a joint optical and X-ray selection
Grandis, Bocquet+21 (2021MNRAS.507.5671G): Simulation-based calibration of weak-lensing masses
Liu+22a (2022A&A...661A...2L): First catalog of eROSITA clusters
Liu+22b (2022A&A...661A...27L): Characterizing eFEDS with simulations
Klein+22 (2022A&A...661A...4K): Optical confirmations of eFEDS clusters
Chiu+22 (2022A&A...661A..11C): First weak-lensing mass calibration of eROSITA clusters
Chiu+23 (2023MNRAS....522...1601C): **First cosmological constraints from eROSTIA clusters**
Bulbul+24 (2024A&A...685A...106B): The eRASS1 cluster catalog
Ghirardini+24 (2024A&A...689A...298G): The eRASS1 cluster cosmology

The Latest Cosmology From eROSITA All-Sky Survey (eRASS)



Why do we care about eFEDS?

- eFEDS probes more low-mass and high-z clusters (because it is deeper than eRASS1)
- The eFEDS selection function is directly measured (complementary to the simulation-anchored calibration in eRASS1)

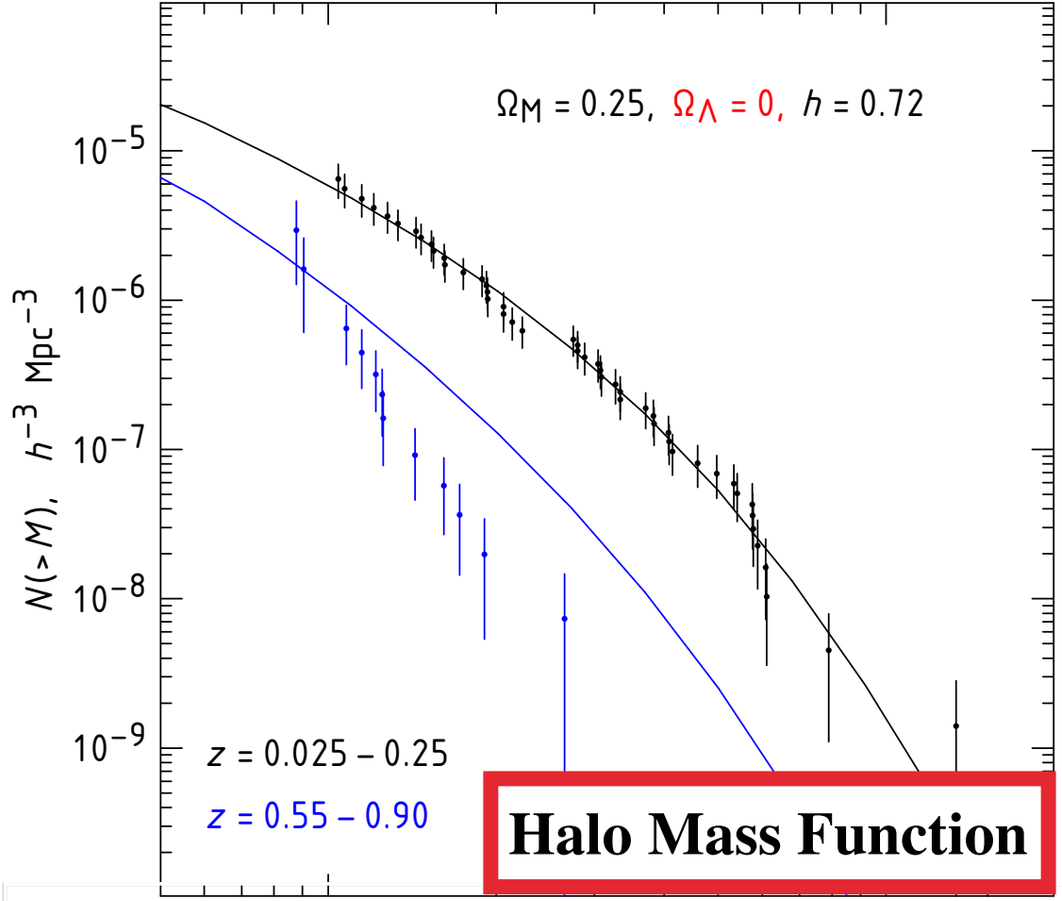
Outlines

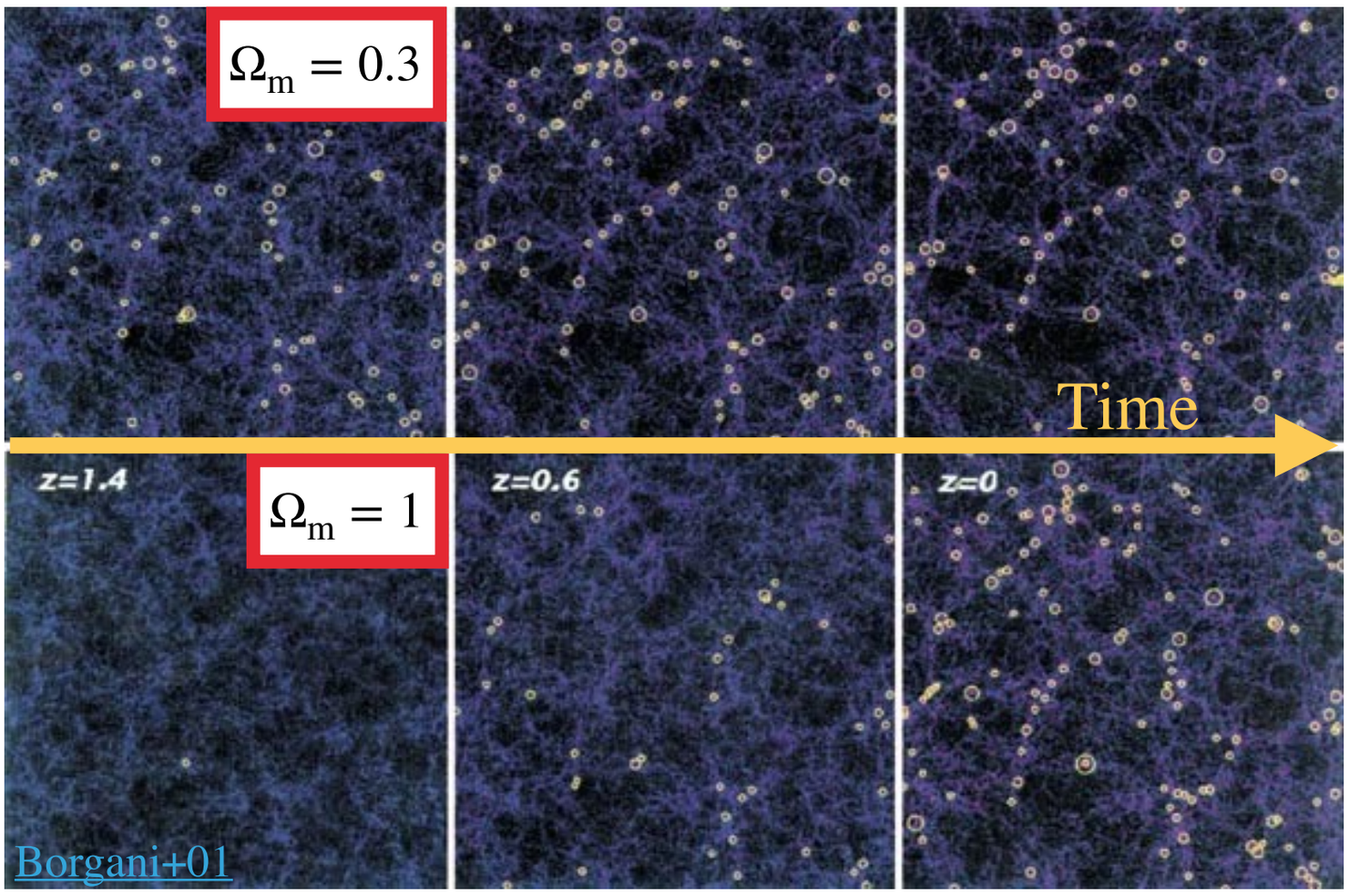
NCKU

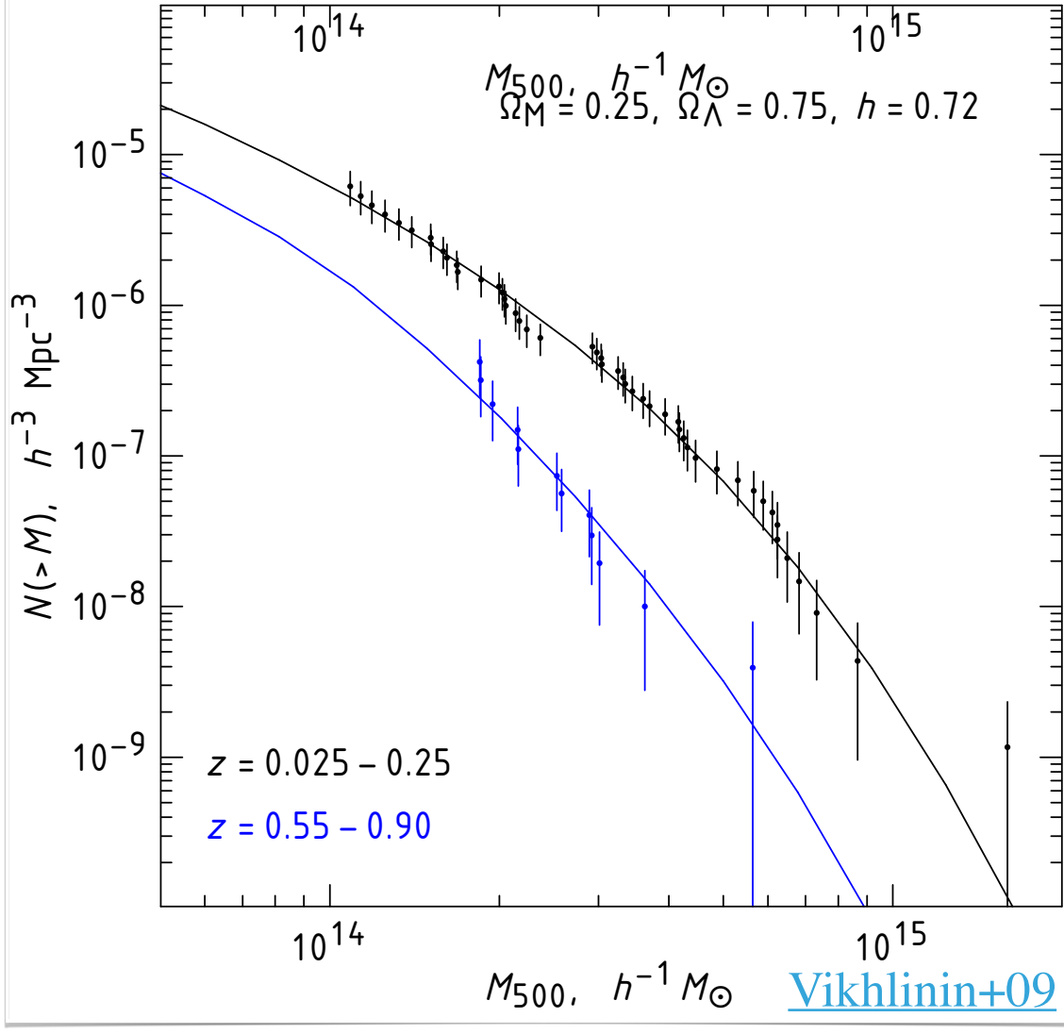
- The frontier of cluster cosmology
- The eROSITA Final Equatorial Depth Survey (eFEDS)
- Cosmological results from eFEDS

Cluster Cosmology

- Galaxy clusters locate at the density peaks of large-scale structures
- Cluster cosmology is rooted in the measurement of the halo mass function

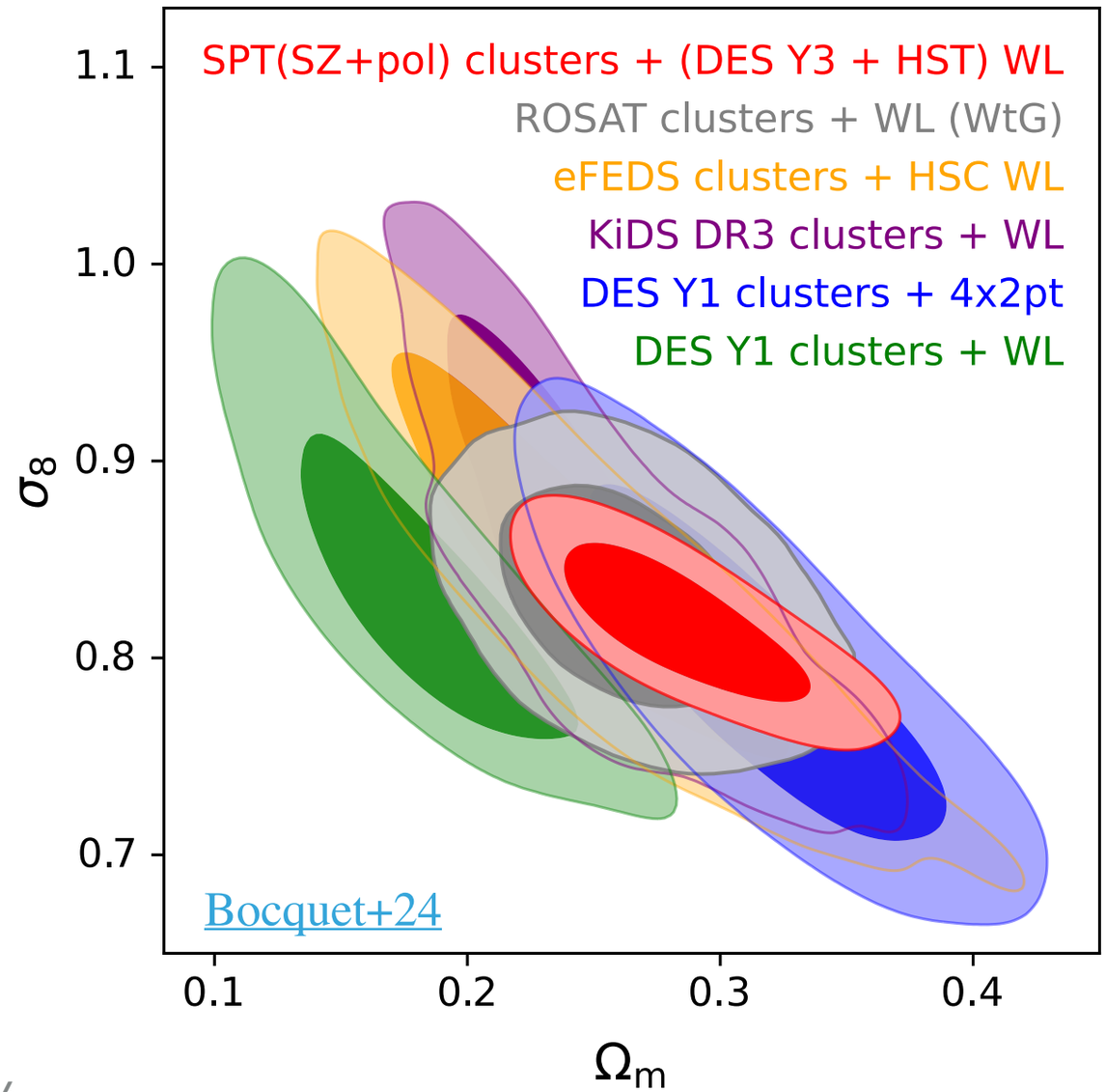


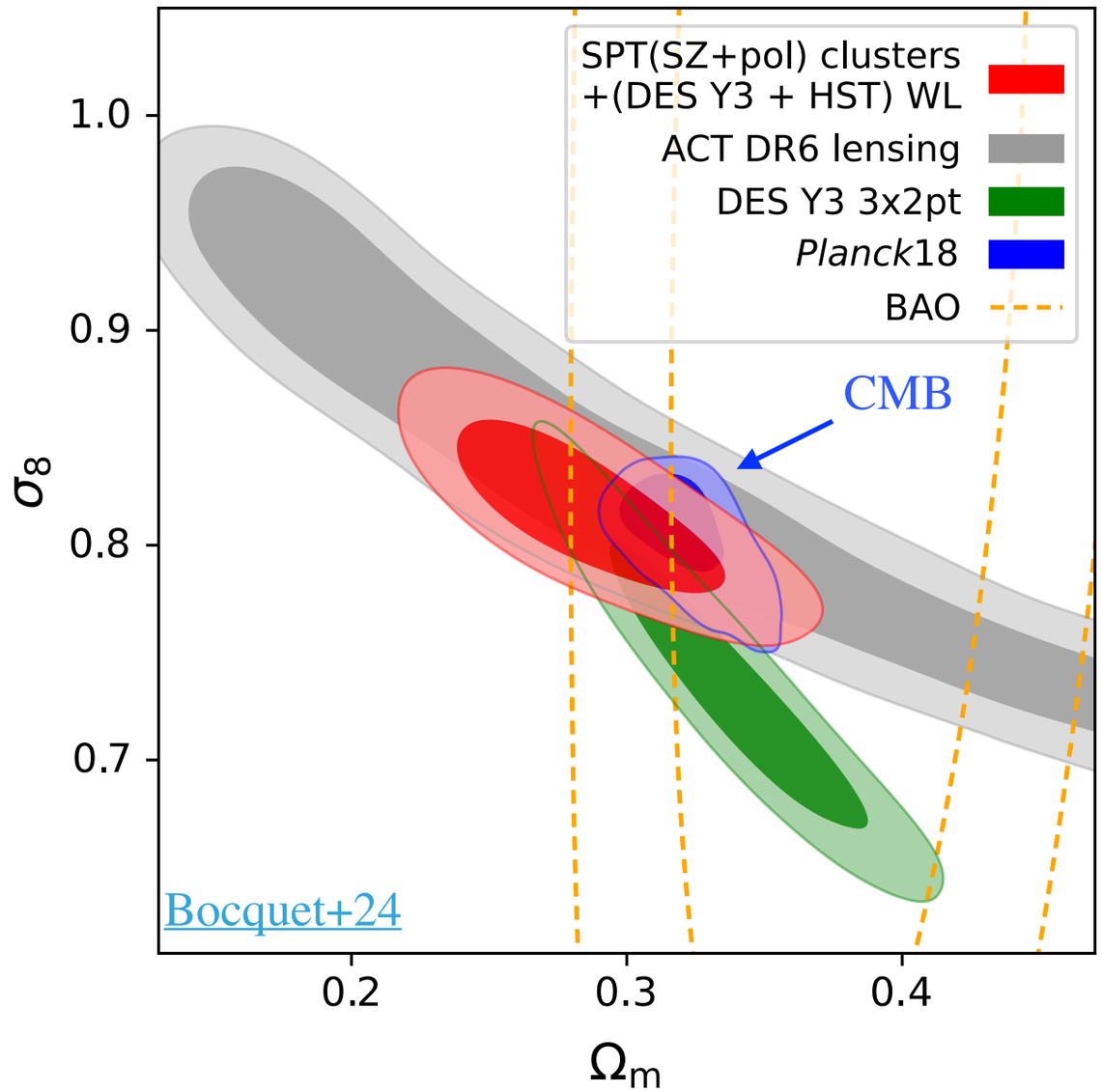




State of the Art

- Cluster cosmology has received great success in multiple wavelengths
- Current sample sizes $\approx 10^3$ clusters (or only small part of the whole sky)
- The cluster abundance remains the most powerful growth-based probe

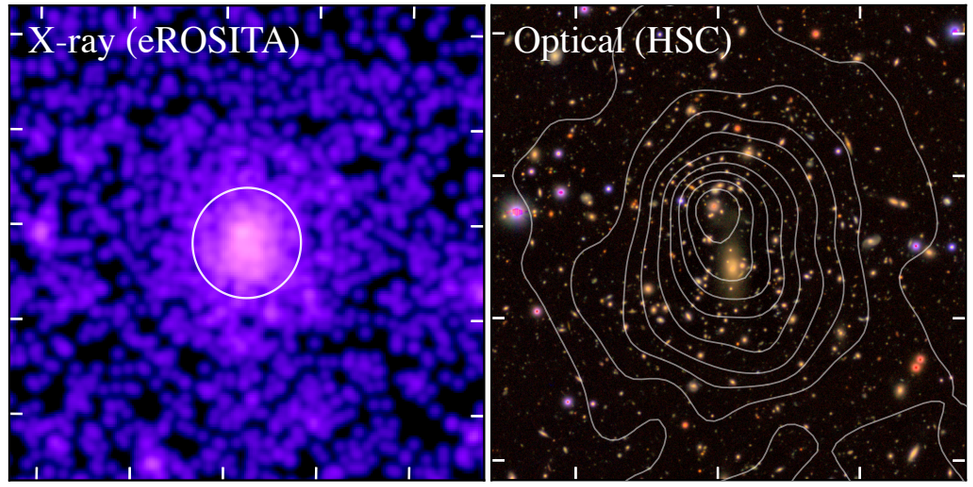




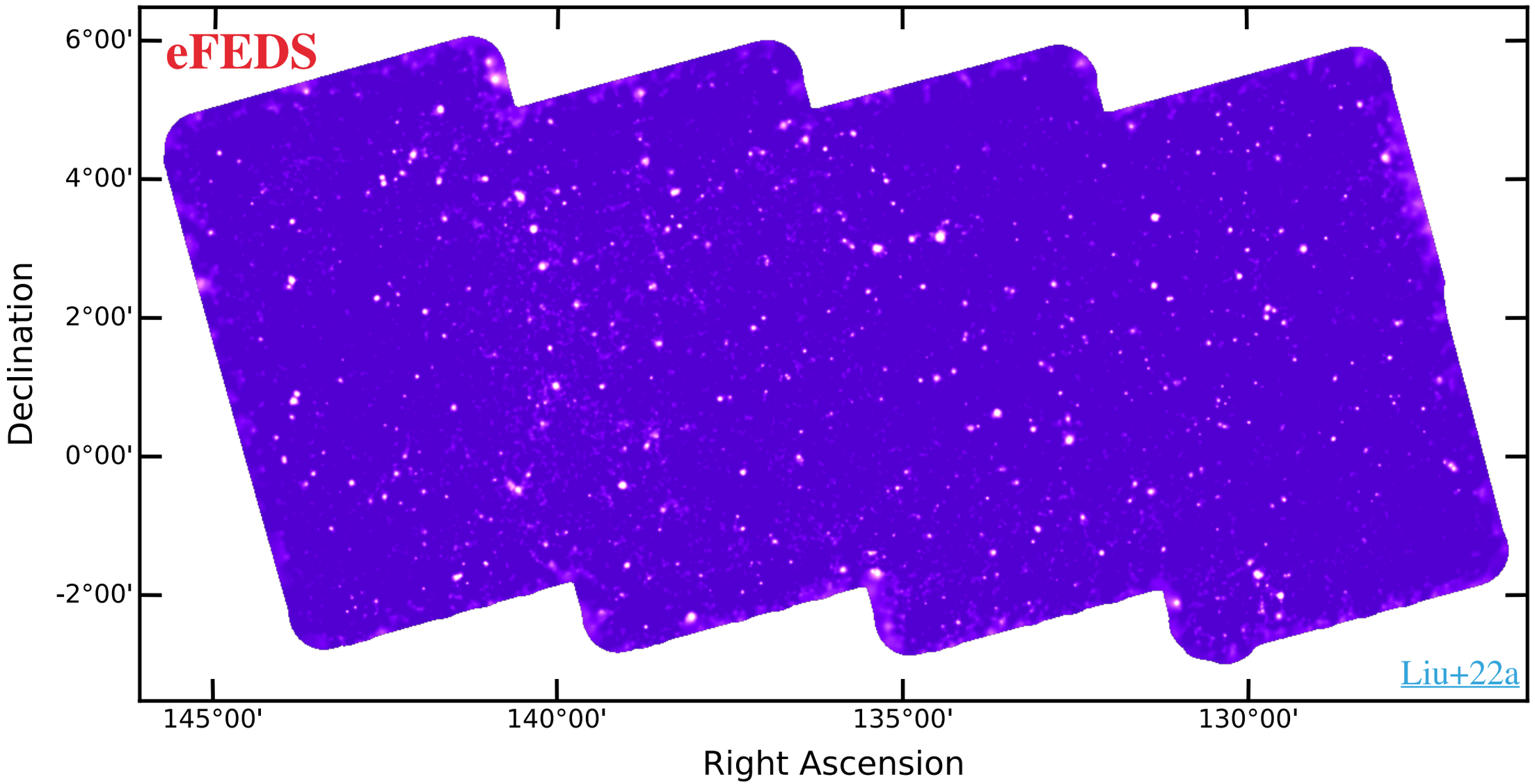
The eROSITA Final-Equatorial Depth Survey (eFEDS)

NCKU

- Area ≈ 140 deg² and the survey final depth
- The sample of 542 clusters constructed in X-rays
- Coverages of the LS and HSC survey
  - ➡ the cluster redshift and WL mass
- The sample is contaminated at a level of ≈ 20 %



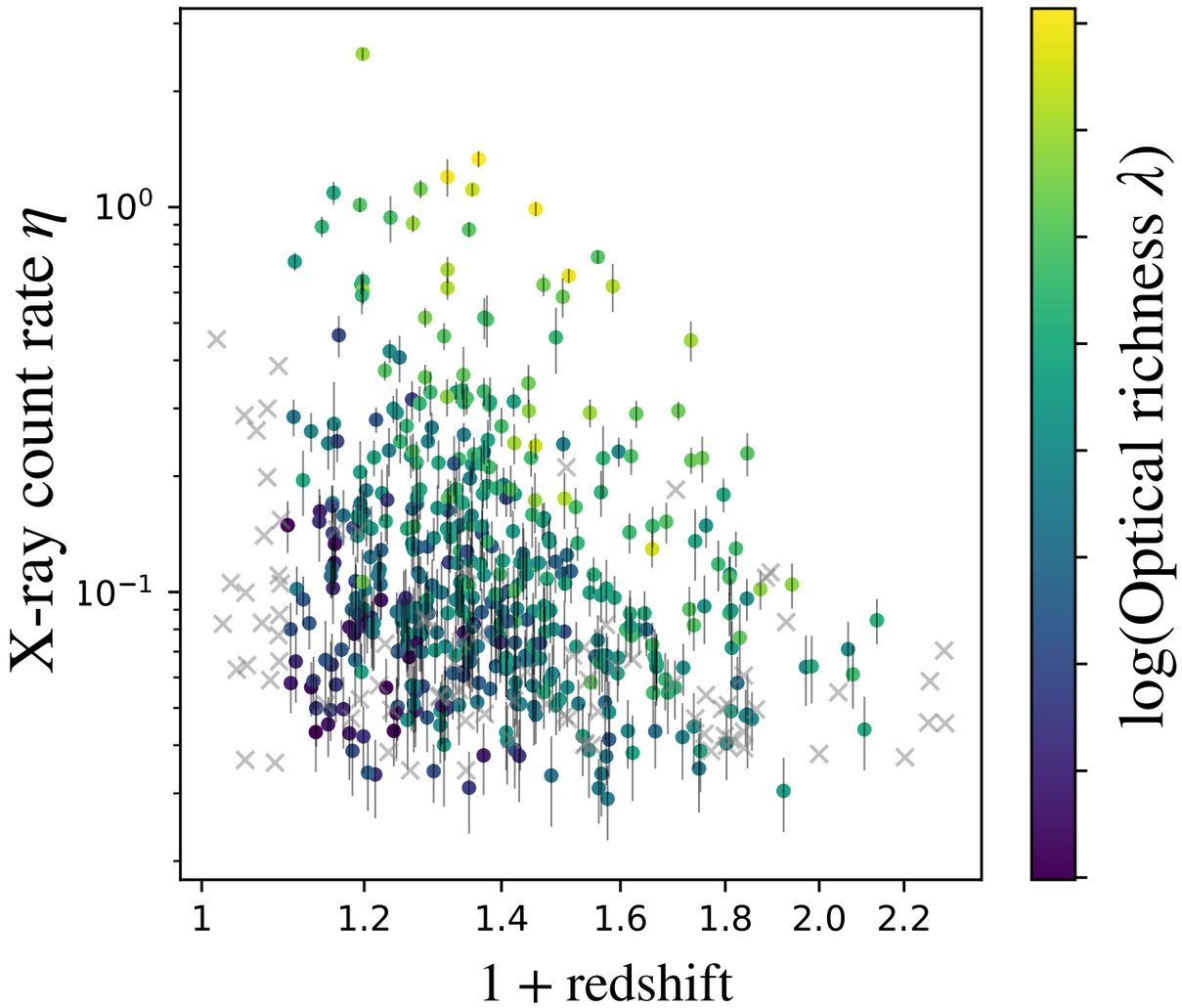
Liu+22a



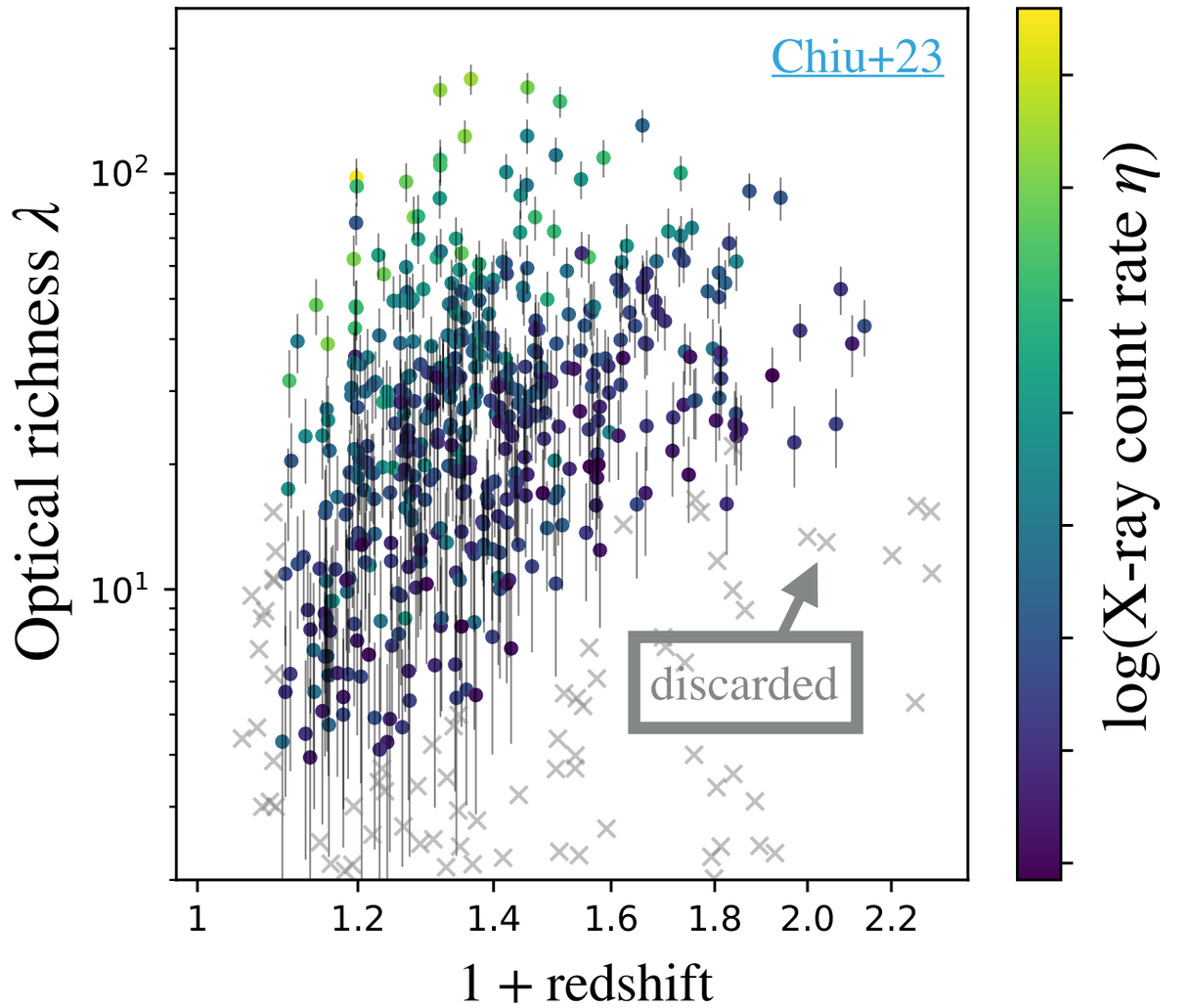
The clusters are selected in X-rays and further confirmed in the optical

➡ **A joint X-ray and optical selection**

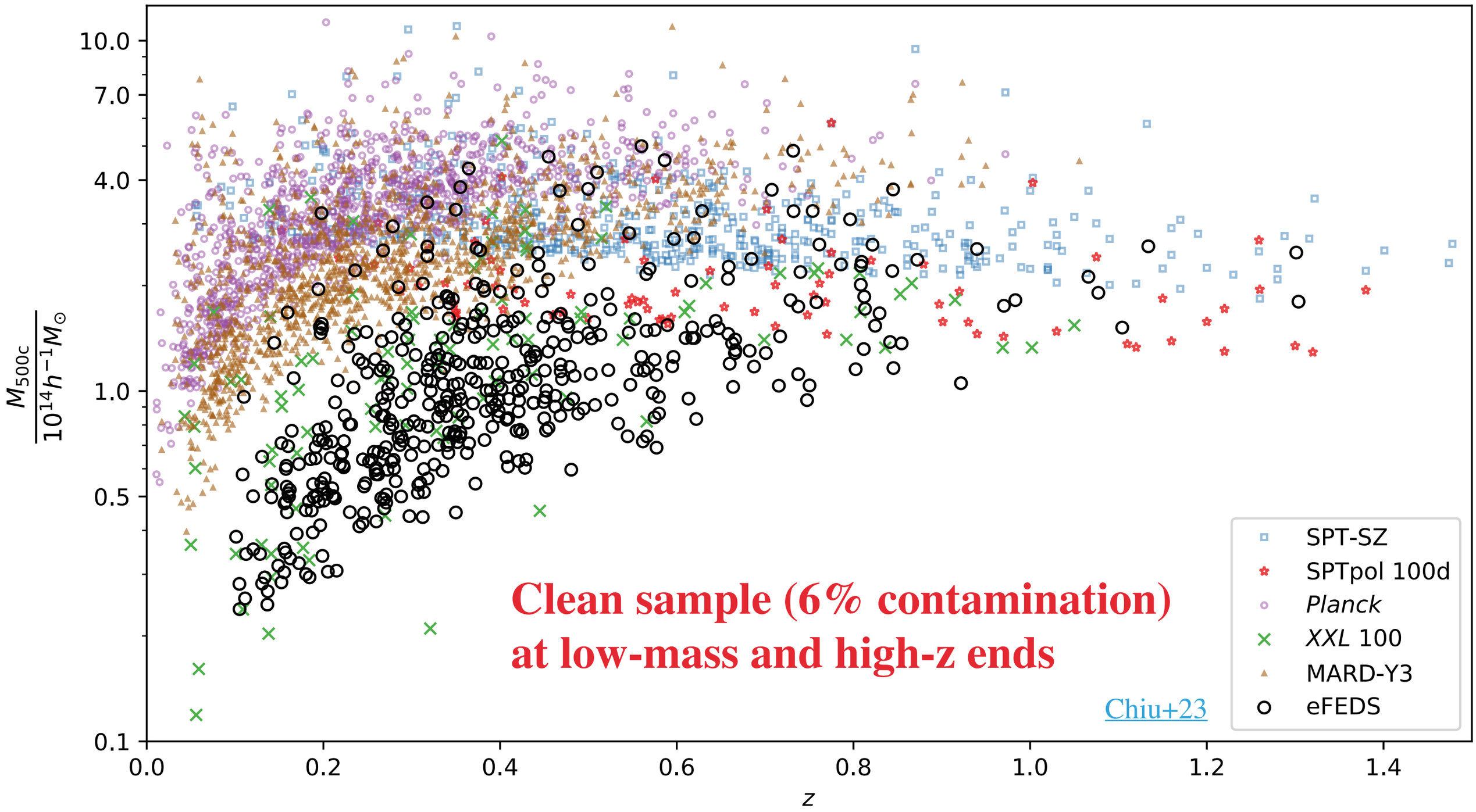
542 ➡ 455 clusters



Contamination 20% (X-ray)
➡ 6% (X-ray+Optical)

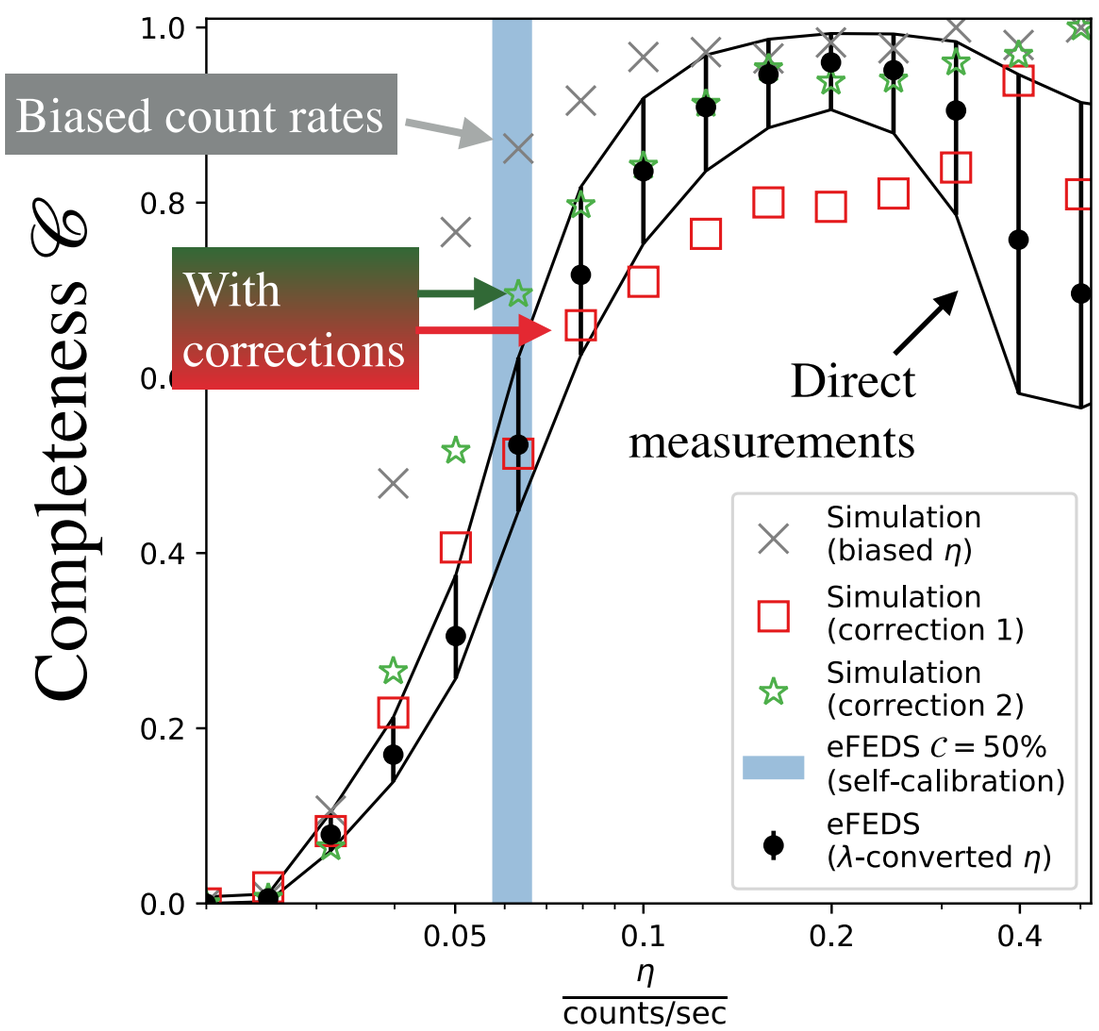


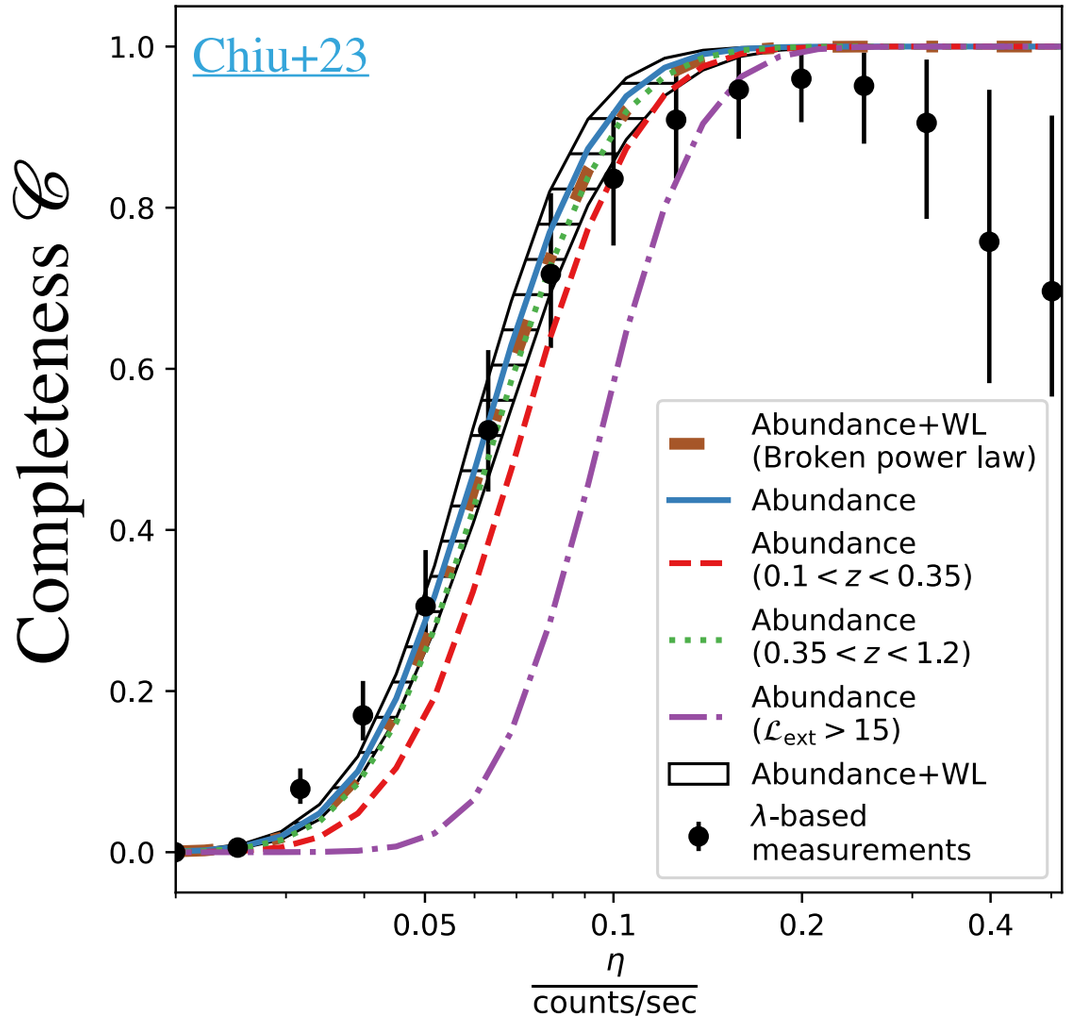
The eFEDS Cluster Sample

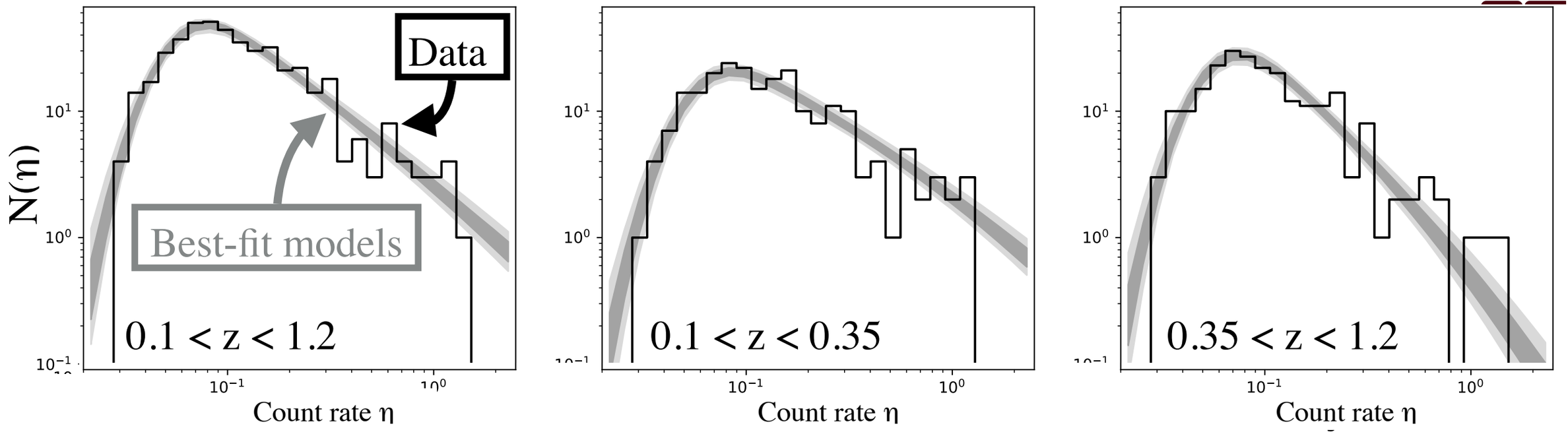


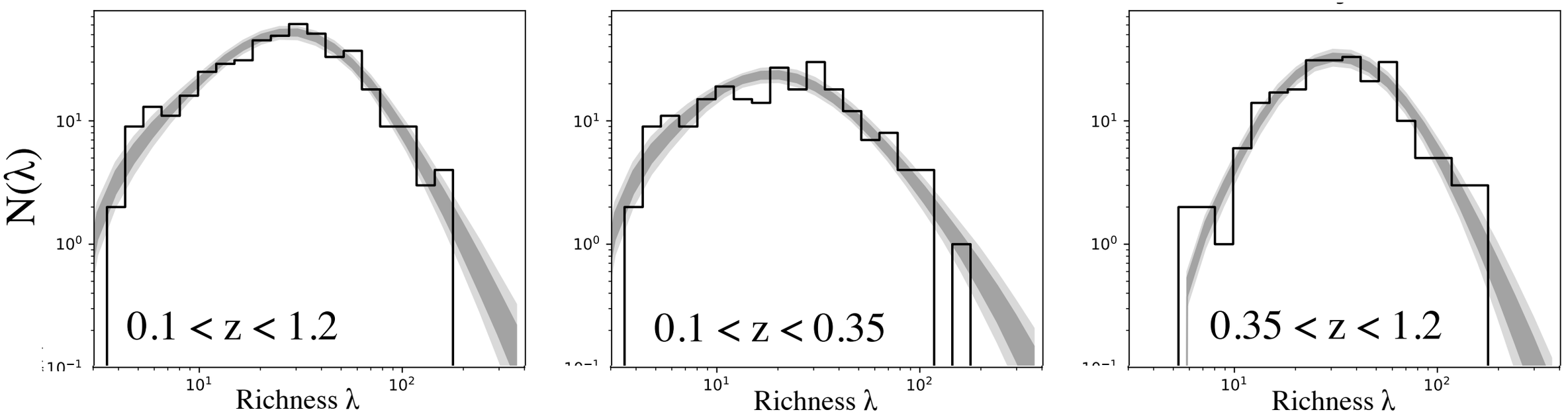
The X-Ray Selection Function

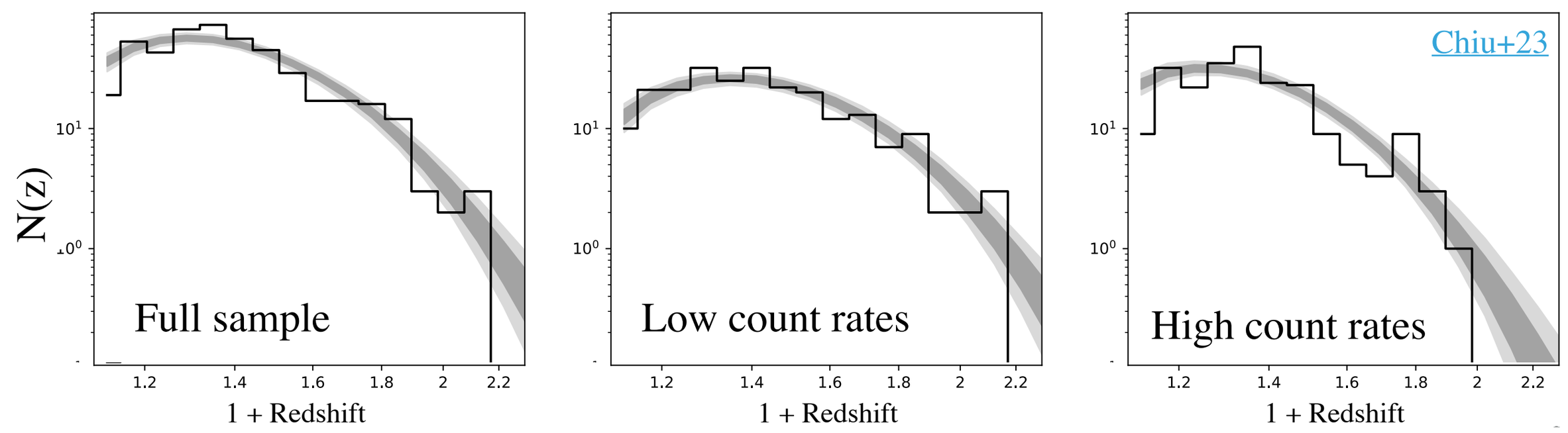
- The selection function ≈ the completeness $\mathscr{C}(\eta)$ as a function of the count rate η
- Counting missing clusters in the point-source (PS) catalog does not work
  - ✗ The count rate η is extracted differently in the PS catalogs
- **The richness λ enables the direct measurement of the completeness $\mathscr{C}(\eta)$**
  - ✓ The richness λ is consistently estimated using the uniform optical survey
  - ✓ Measuring cluster numbers $N(\lambda)$ in both cluster and PS catalogs
  - ✓ Deriving the completeness $\mathscr{C}(\lambda)$ in richness
  - ✓ Converting the completeness $\mathscr{C}(\lambda) \rightarrow \mathscr{C}(\eta)$ by the $\lambda - \eta$ relation





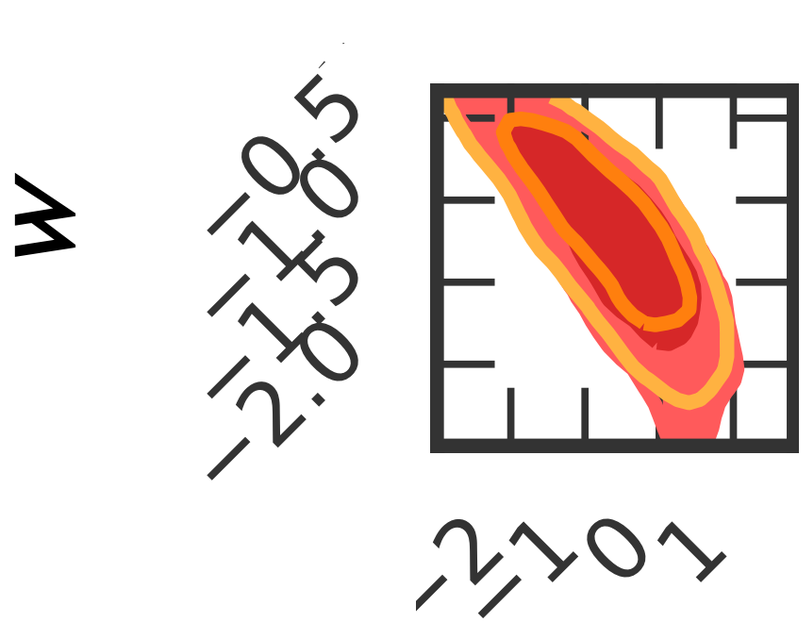

Data
Best-fit models
0.1 < z < 1.2
0.1 < z < 0.35
0.35 < z < 1.2
N(η)
Count rate η


0.1 < z < 1.2
0.1 < z < 0.35
0.35 < z < 1.2
N(λ)
Richness λ

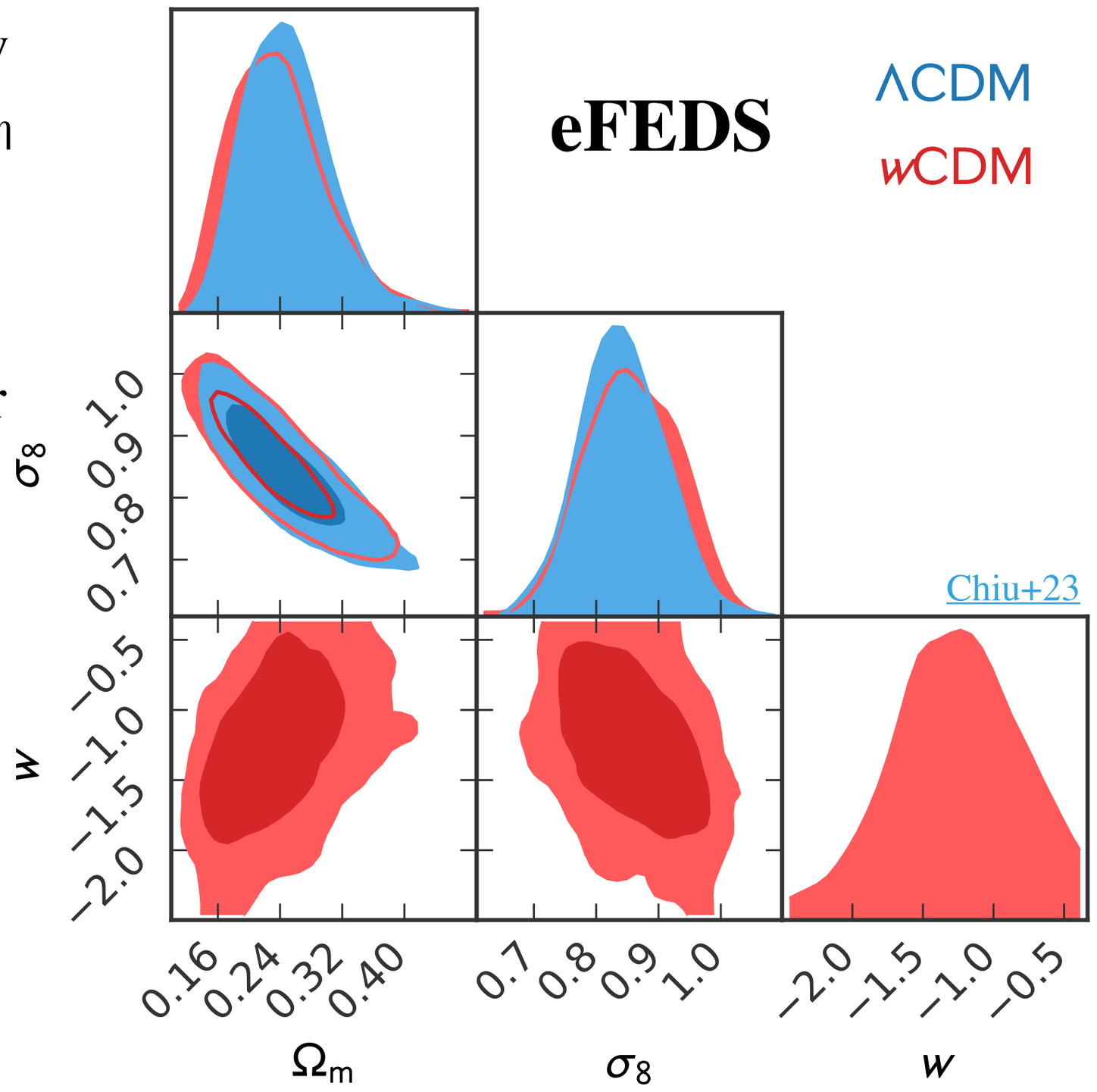

Chiu+23
Full sample
Low count rates
High count rates
N(z)
1 + Redshift

eFEDS Cosmological Constraints

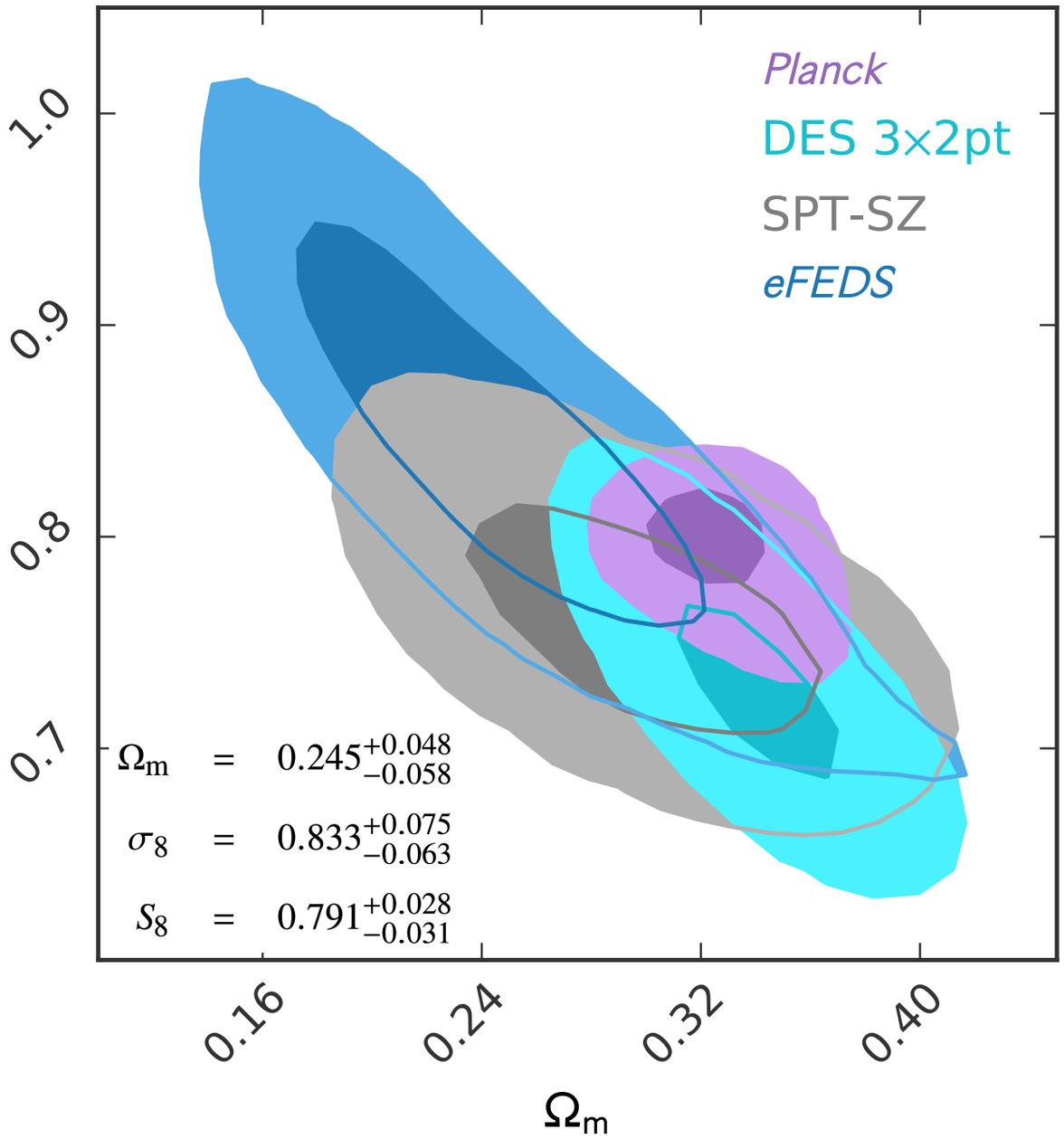
- (Ω_m, σ_8) are not sensitive to w
- Degeneracy between w and γ_η
  ➡ Must improve high-z WL calibration
- Including w ➡ no significant deviation from the self-similar redshift prediction



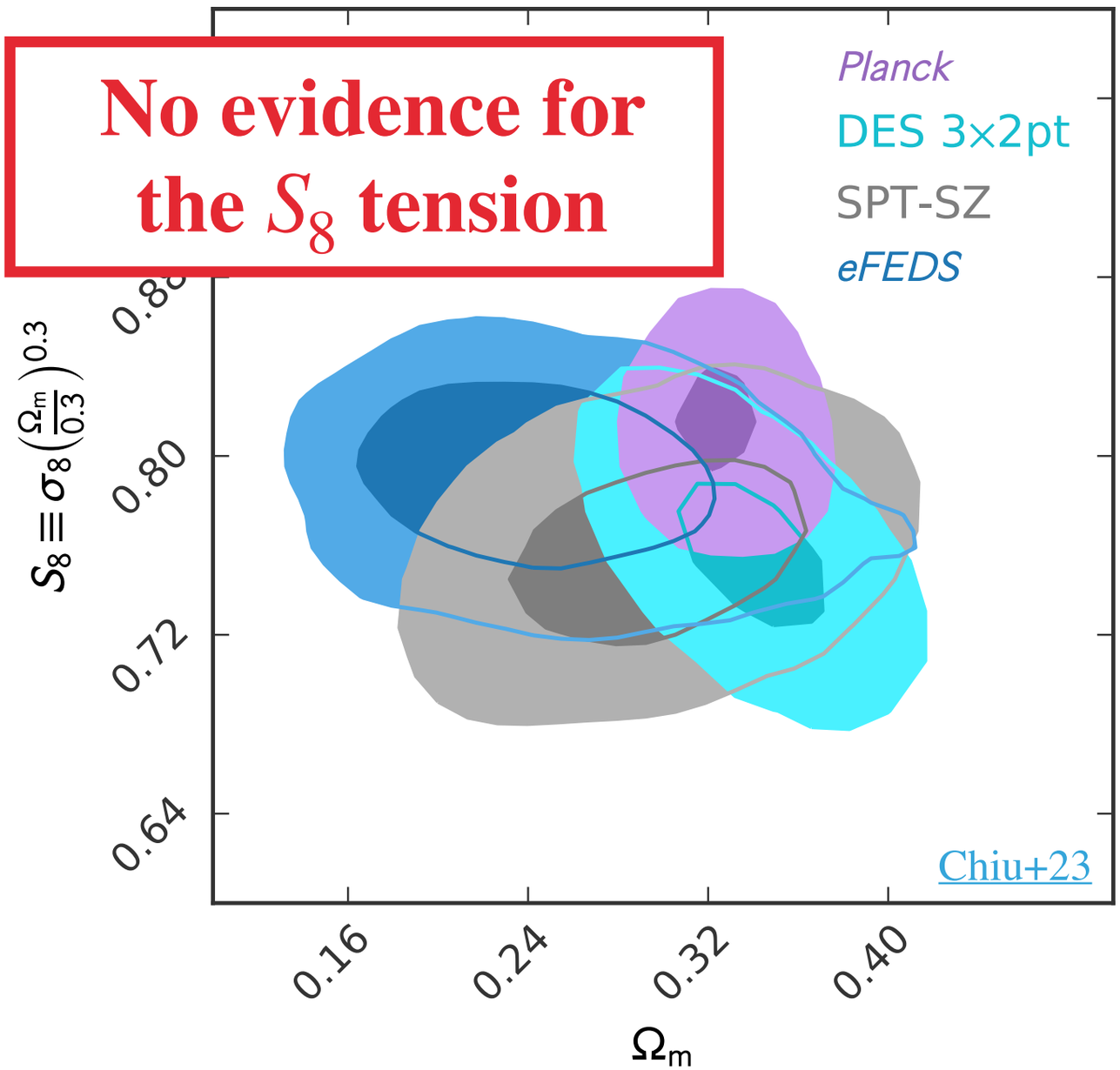
Redshift scaling of the count rate γ_η



The Flat ΛCDM Cosmology

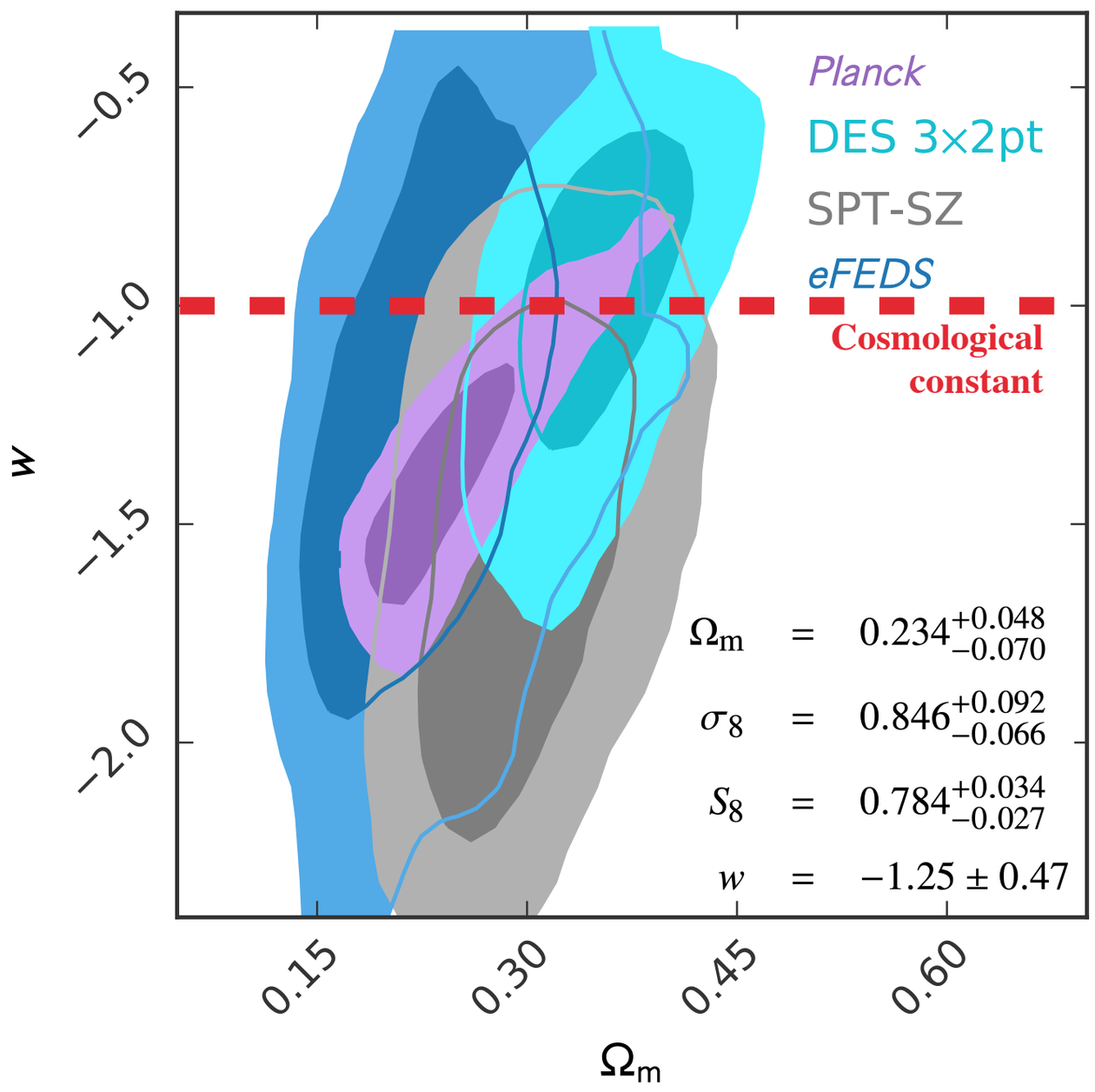


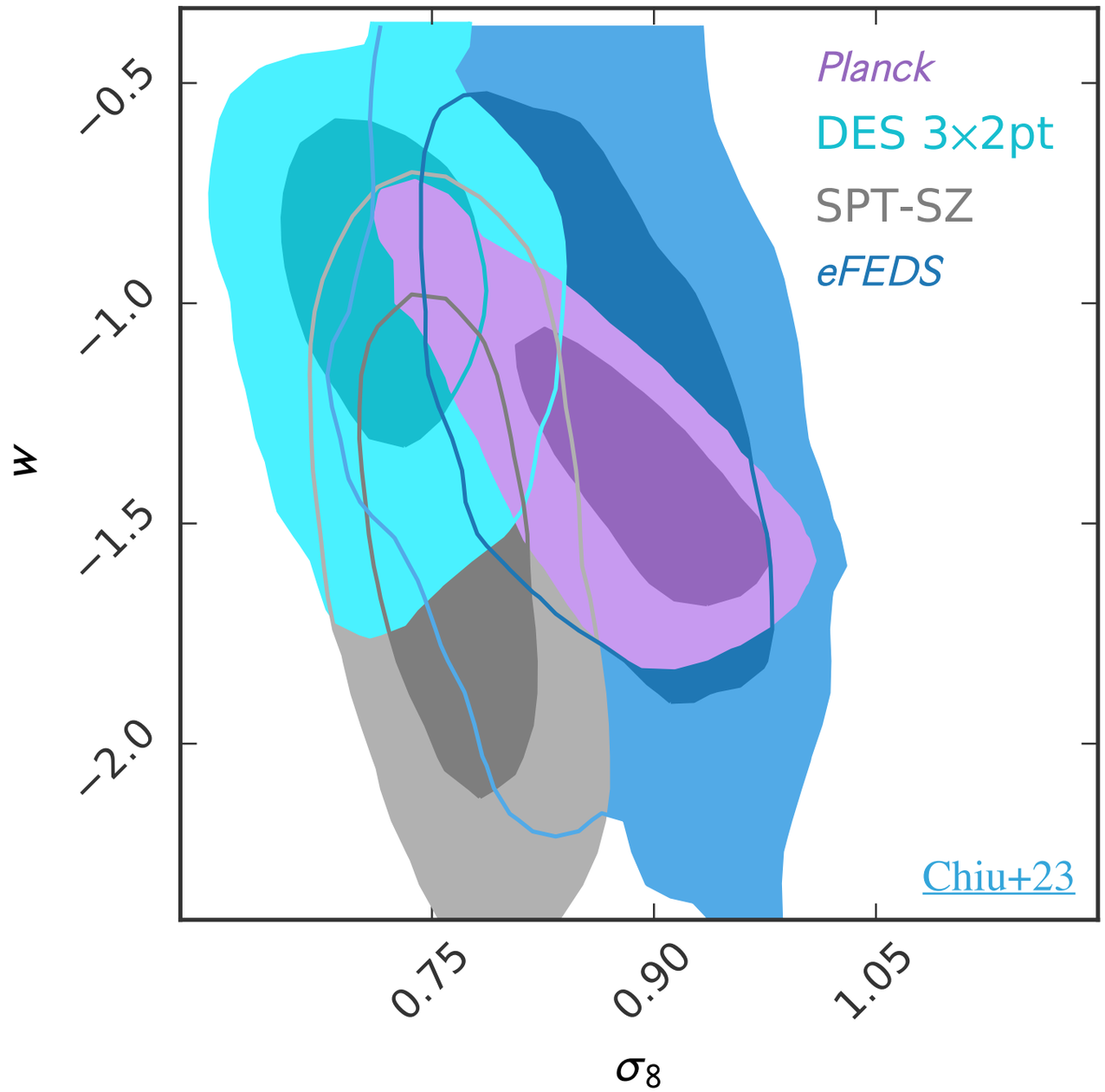
No evidence for the S_8 tension



Consistency at ≲ 1.2σ

The Flat *w*CDM Cosmology





Consistency at ≲ 1σ

Conclusions

NCKU

- We present the eFEDS cosmological constraints with the measured selection function
- The results are in excellent agreement (≲1.2σ) with other probes, e.g., Planck CMB
- No clear evidence for the S_8 tension between eFEDS and CMB

I also have a poster!

Back-Up Slides

Modelling in a Nut Shell

$$\frac{\mathrm{d}N(\mathcal{O}, z\,|\,\mathbf{p})}{\mathrm{d}\mathcal{O}\mathrm{d}z} = \int \mathrm{d}M\, \mathscr{C}\left(\mathcal{O}, z\right) P(\mathcal{O}\,|\,M, z, \mathbf{p}) \frac{\mathrm{d}N(M, z\,|\,\mathbf{p})}{\mathrm{d}M\mathrm{d}z}$$

Selection — WL mass calibration

- The clusters are selected in X-rays and further confirmed in the optical
  - ➡ **Joint X-ray and optical selection**
- Modelling the cluster numbers as a function of the observables
  $\mathcal{O} = \left\{\text{Xray count rate } \eta, \text{optical richness } \lambda\right\}$
- Uniform optical follow-ups
  - ✓ Optical richness λ ➡ **A direct measurement of the selection**
  - ✓ High-quality HSC WL ➡ **Mass calibration out to $z \approx 1.3$**

The HSC WL Mass Calibration

Simulation-based calibration accounting for systematics (Grandis+21):

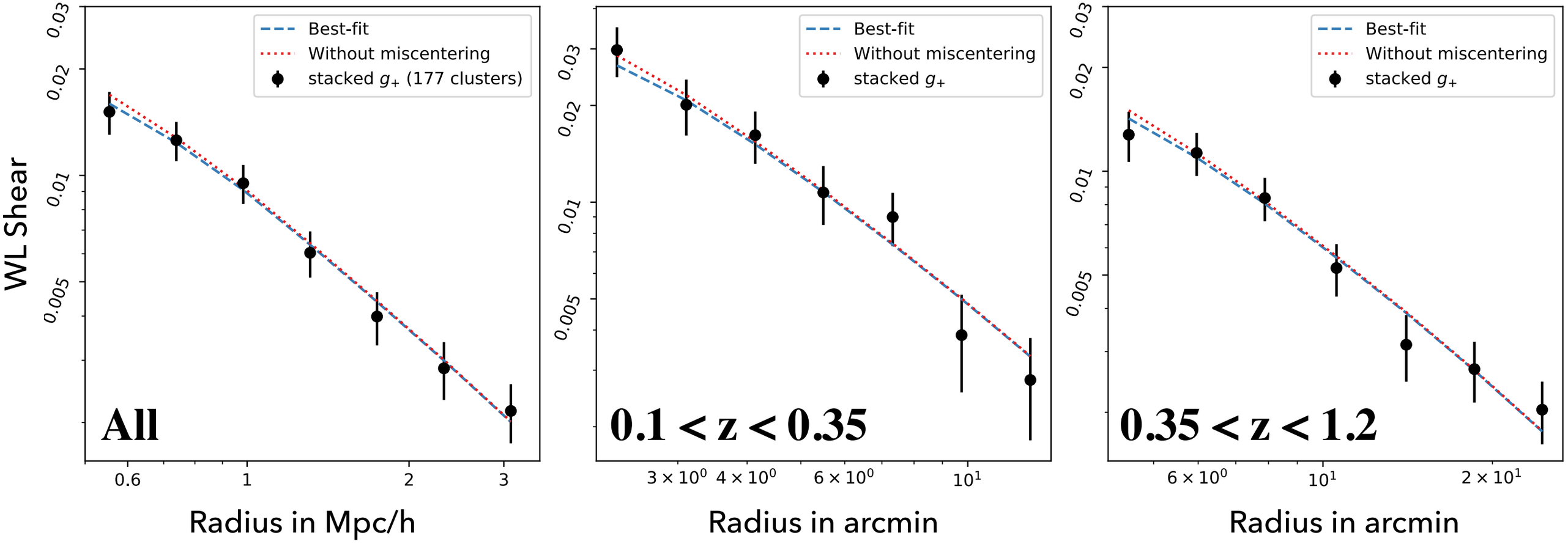
- The calibration bias of the shape measurement
- The cluster member contamination
- The photo-z bias
- The miscentering of X-ray centers
- The misfitting of WL profiles

The weak-lensing mass bias

$$b_{\rm WL} \equiv \frac{M_{\rm WL}}{M_{500,c}} = 0.903 \pm 0.03$$

at $M_{500c} = 2 \times 10^{14} h^{-1} M_\odot$

Chiu+22, Chiu+23



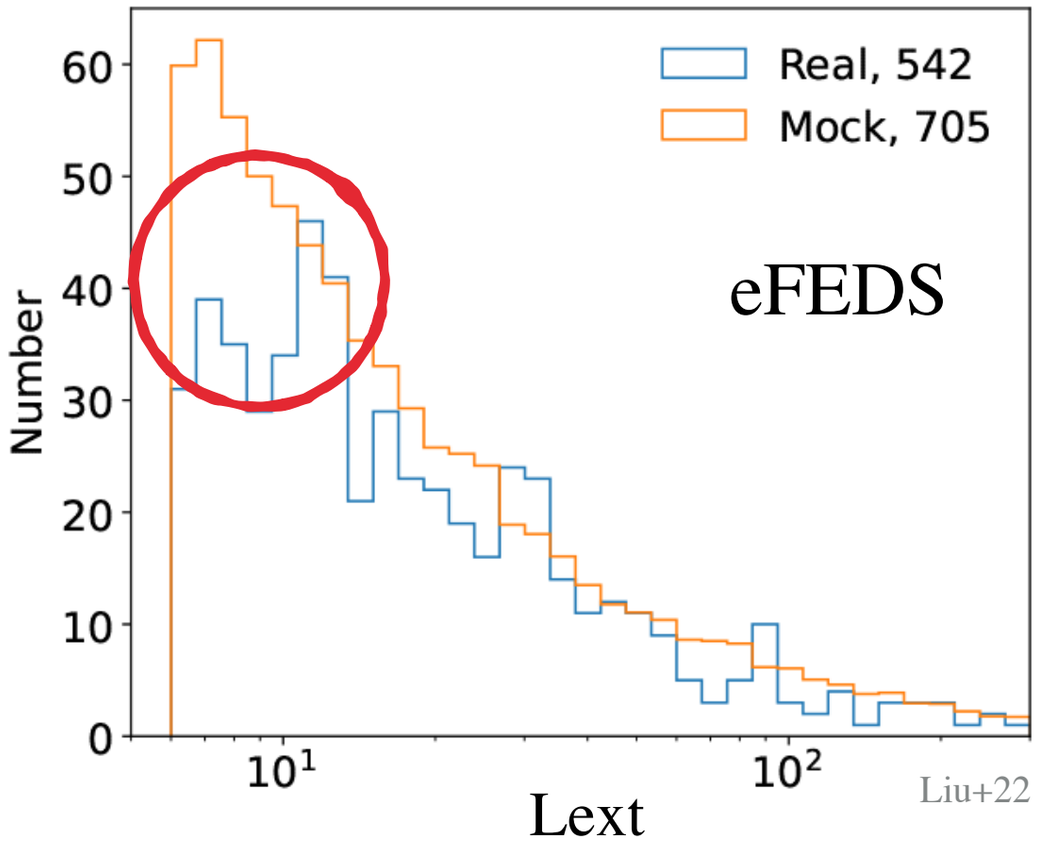
The Inconsistency Between the Data and Simulations

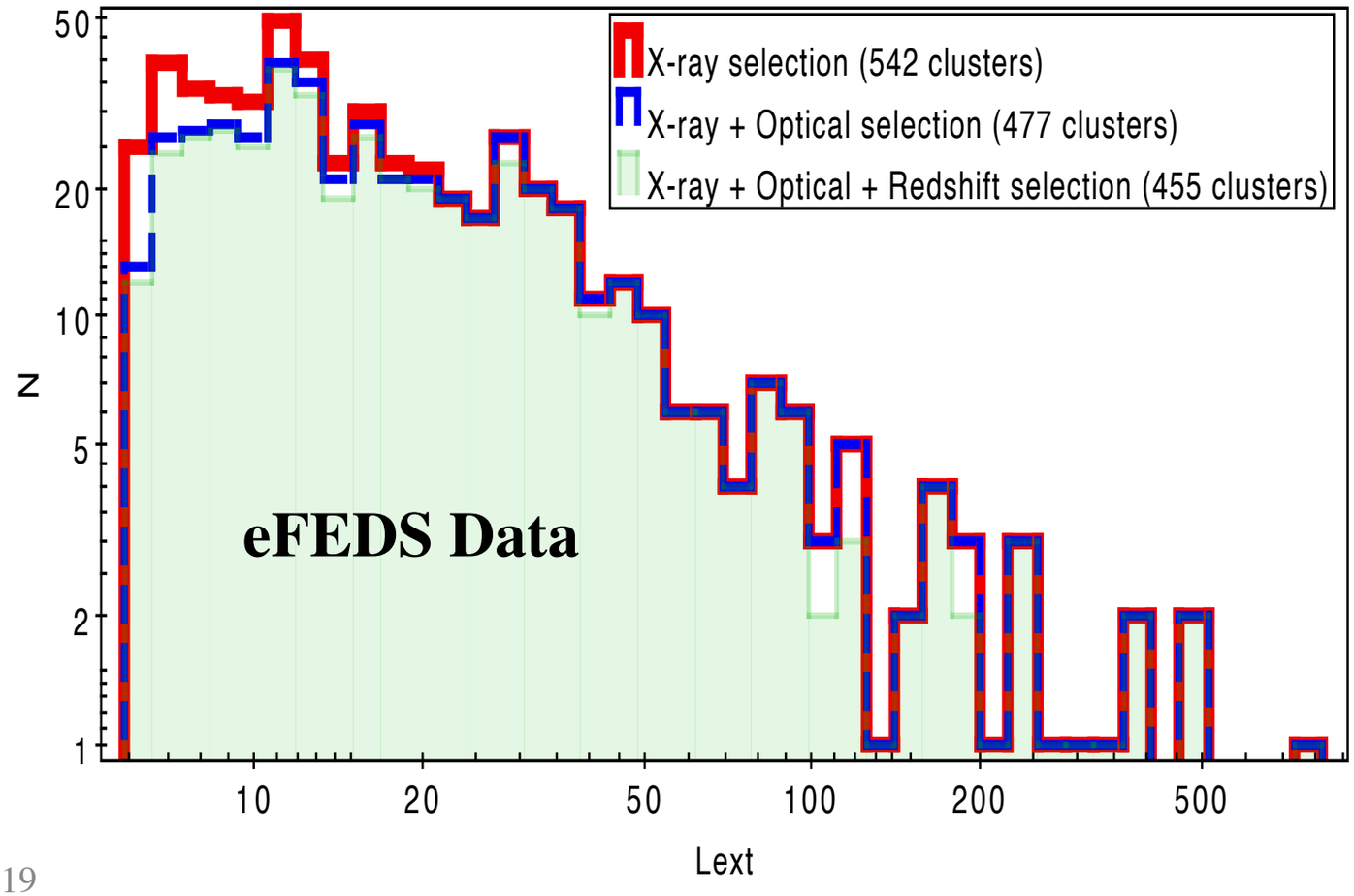
A deficit seen in the low L_{ext} end of data

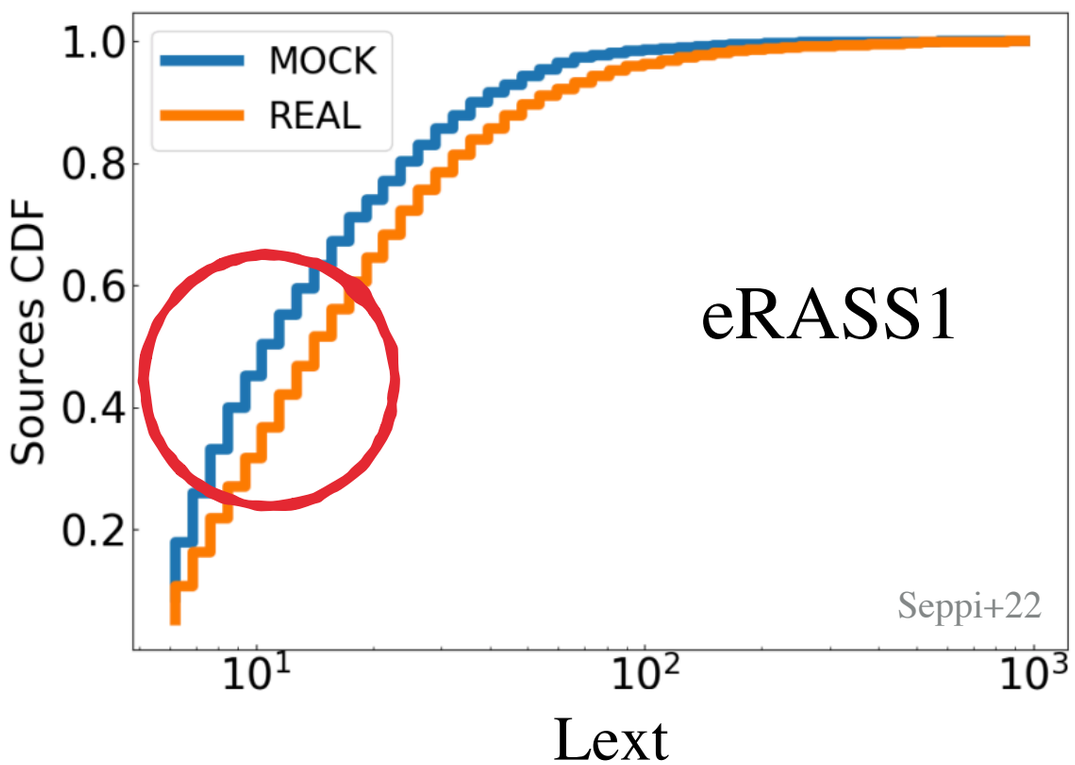
◉Low L_{ext} ➡ Low count rate SNR ➡ Faint clusters ➡ Low-mass clusters

◉Incomplete samples/X-ray physics in the sims?

The sim-inferred modelling might be limited to bright clusters ➡ A much smaller sample







The Broken Power-Law Count Rate Relation

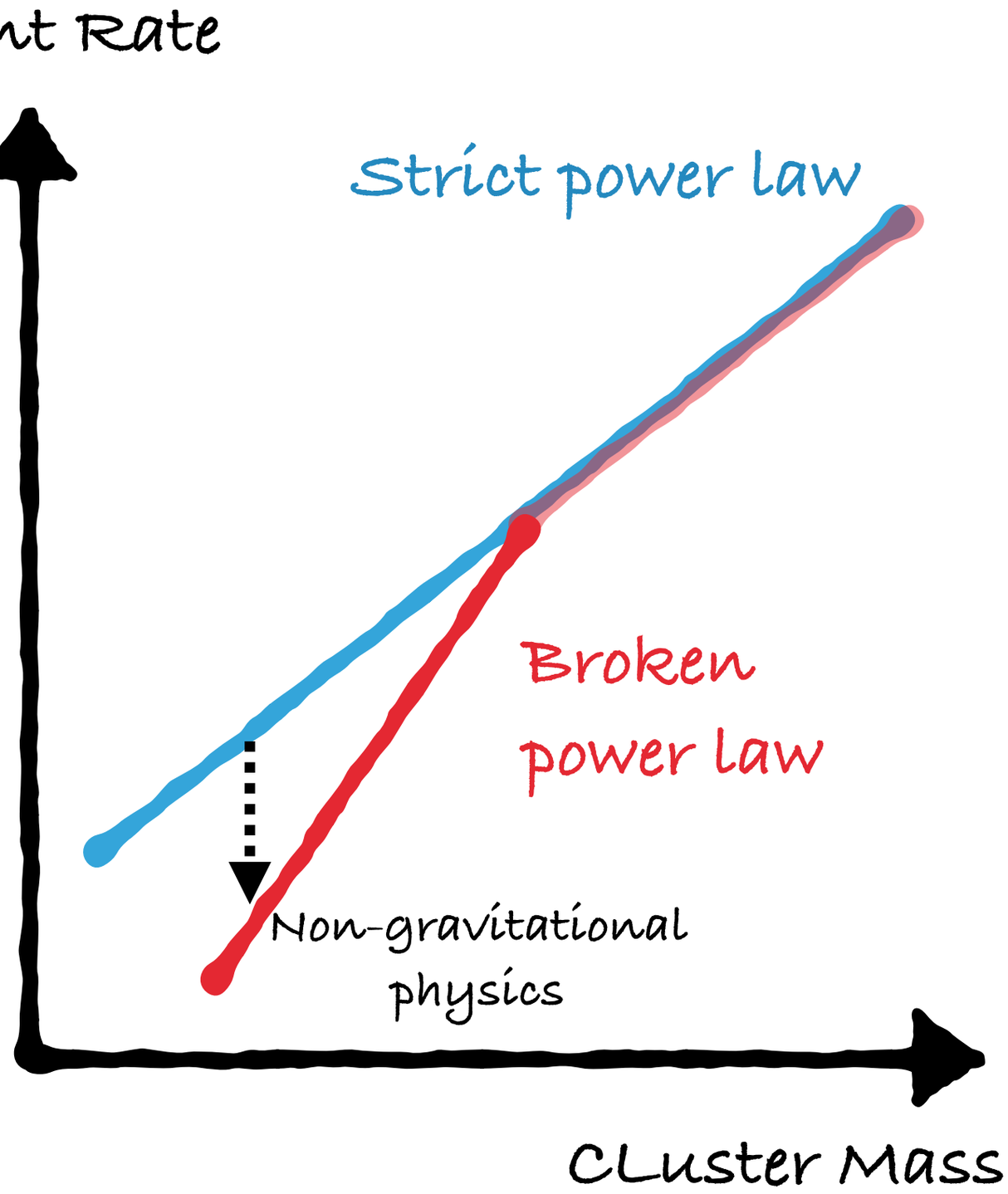
The deficit at low L_{ext} could be explained by a **broken power law** in the count rate-mass relation

◉Low-mass clusters have less ICM and hence lower X-ray fluxes with respect to massive clusters

$$\left\langle \ln\left(\frac{\eta}{\text{counts/sec}}\middle| M, z\right)\right\rangle\Big|_{\text{broken}} = \left\langle \ln\left(\frac{\eta}{\text{counts/sec}}\middle| M, z\right)\right\rangle + \left(\left(B_\eta - B_{\text{grp}}\right)\times\Delta\right)\times\ln\left(1+\left(\frac{M}{M_{\text{grp}}}\right)^{\frac{-1}{\Delta}}\right)$$

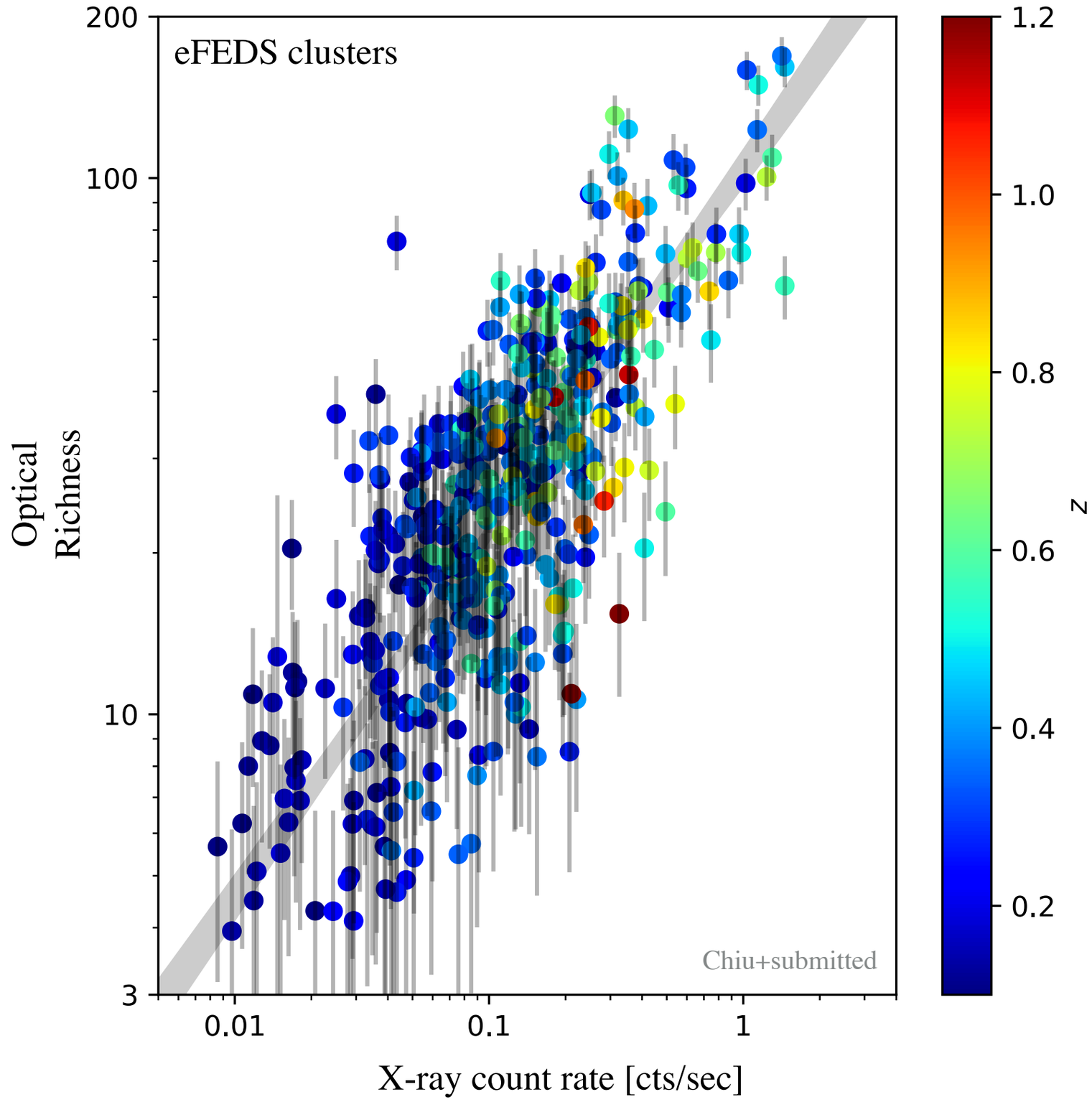
$B_\eta = B_{grp}$: strict power law

$B_\eta < B_{grp}$: broken power law

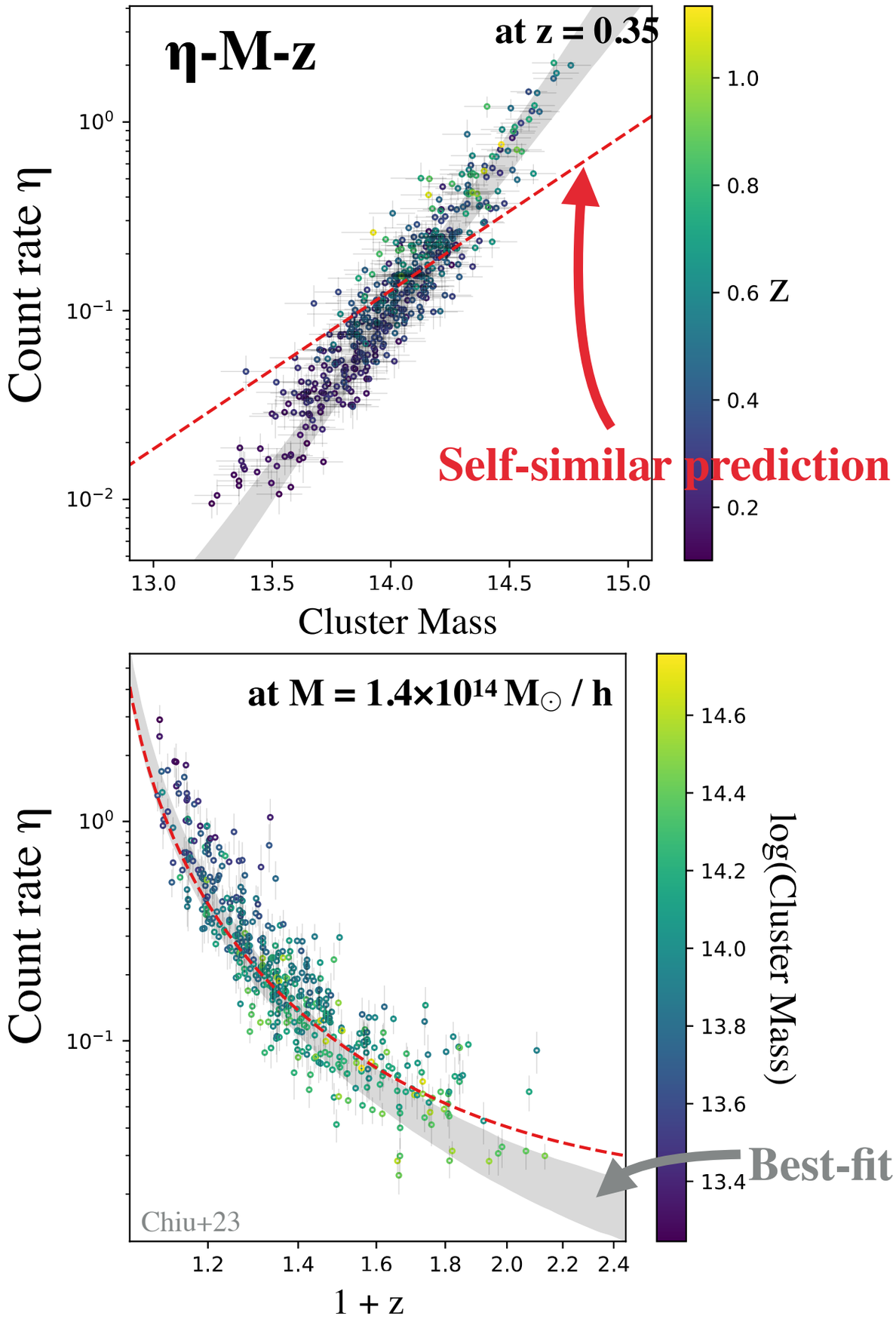


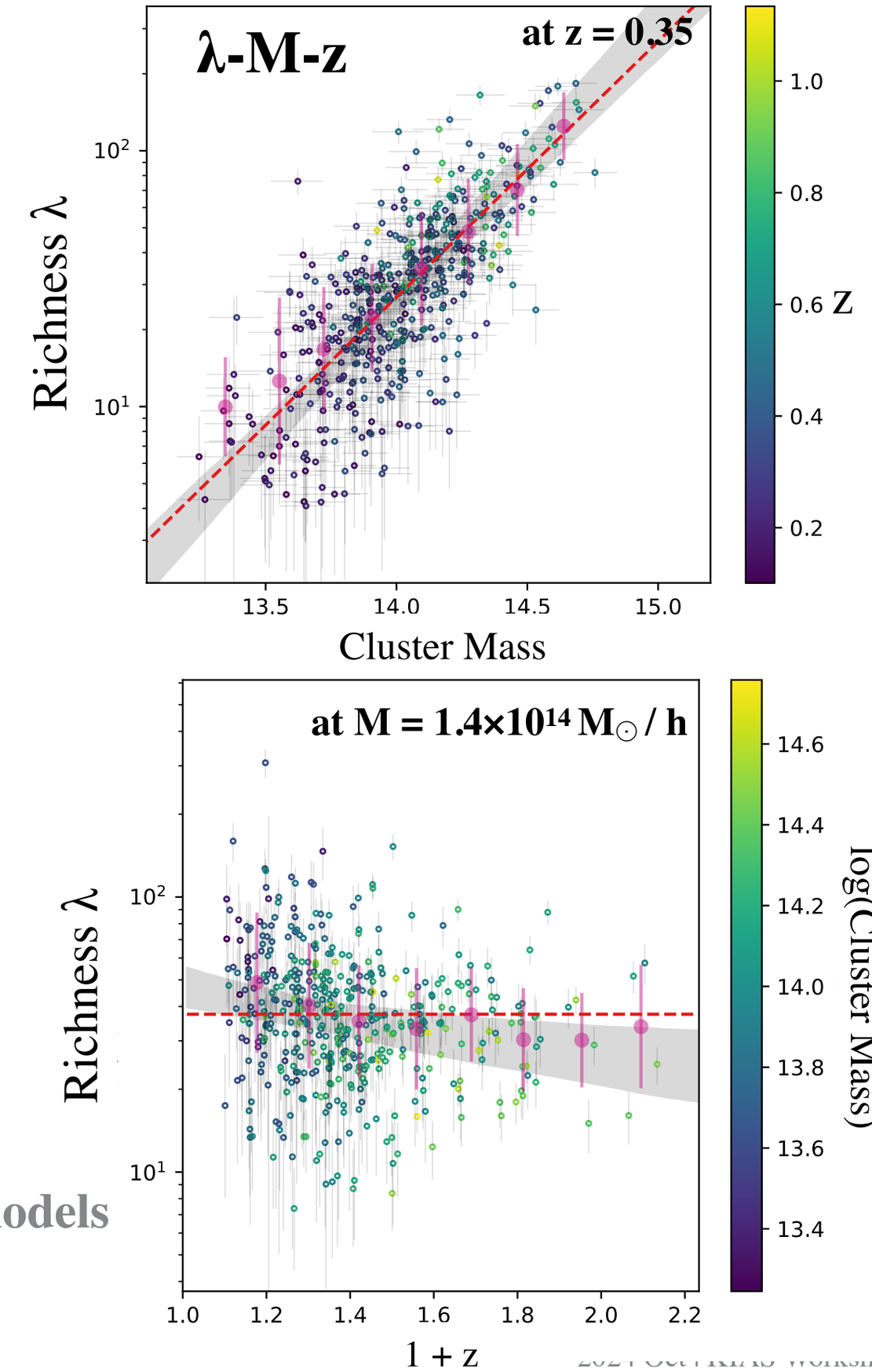
The Richness-to-Rate Relation

- comp(λ) → comp(η)
- Well described by a power law with scatter



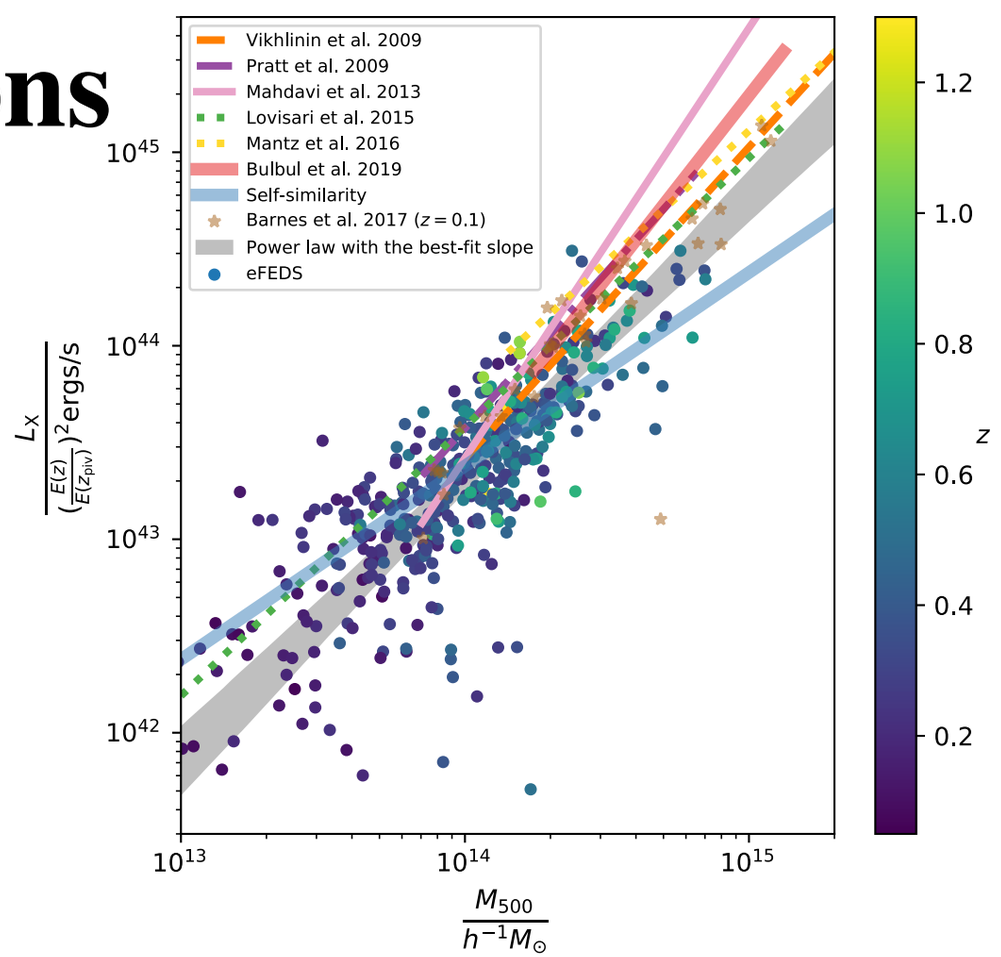
Best-Fit Scaling Relations

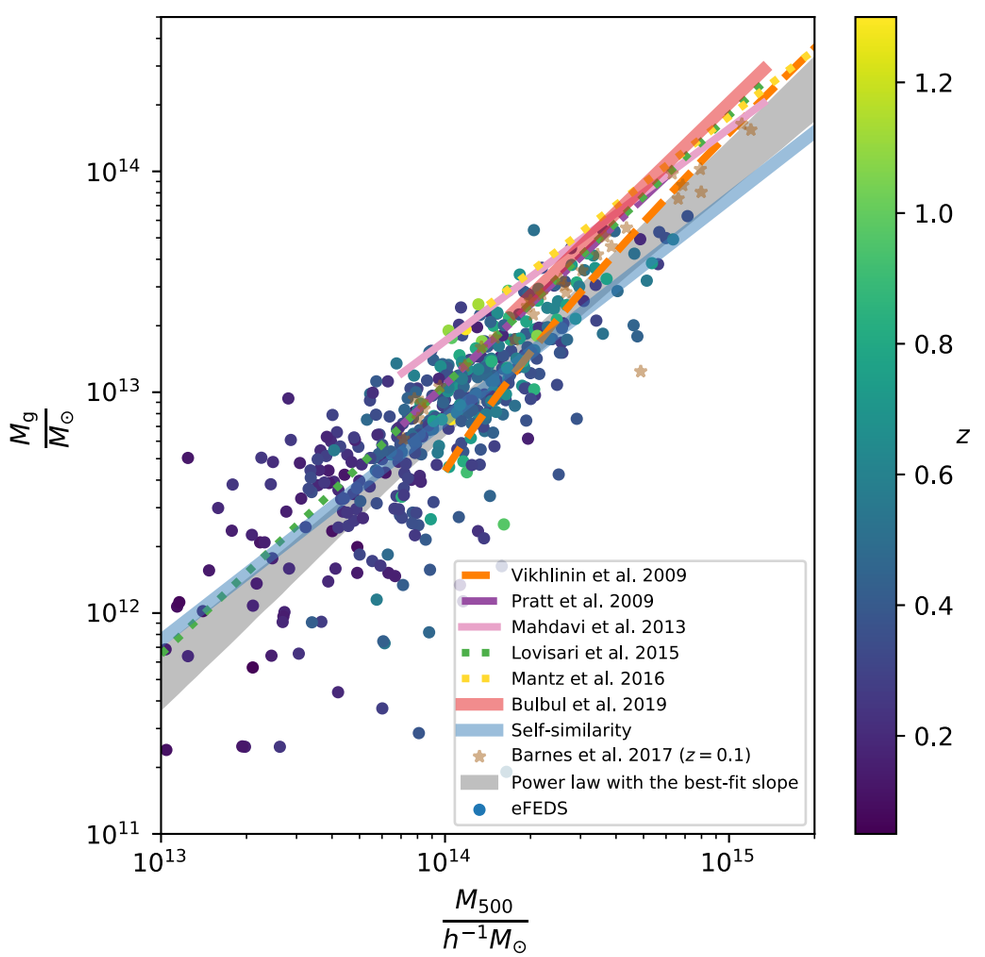


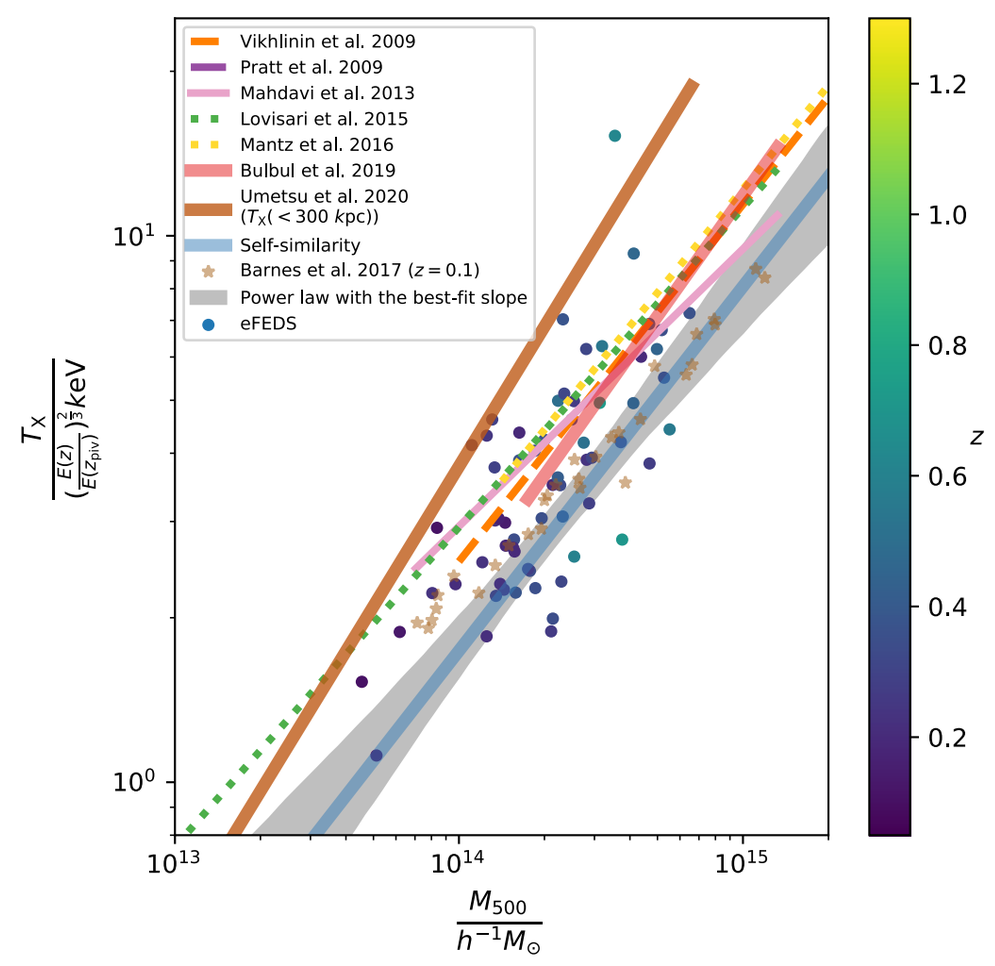


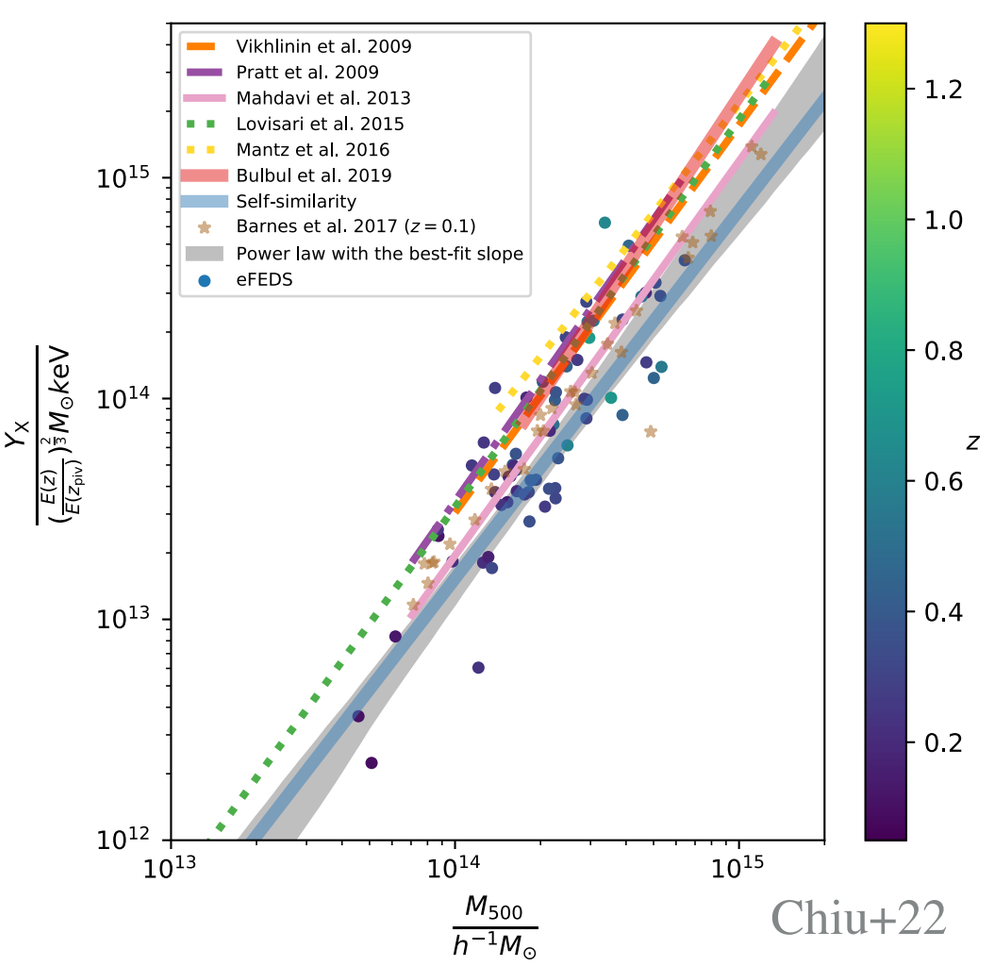
Best-fit models

Comparisons



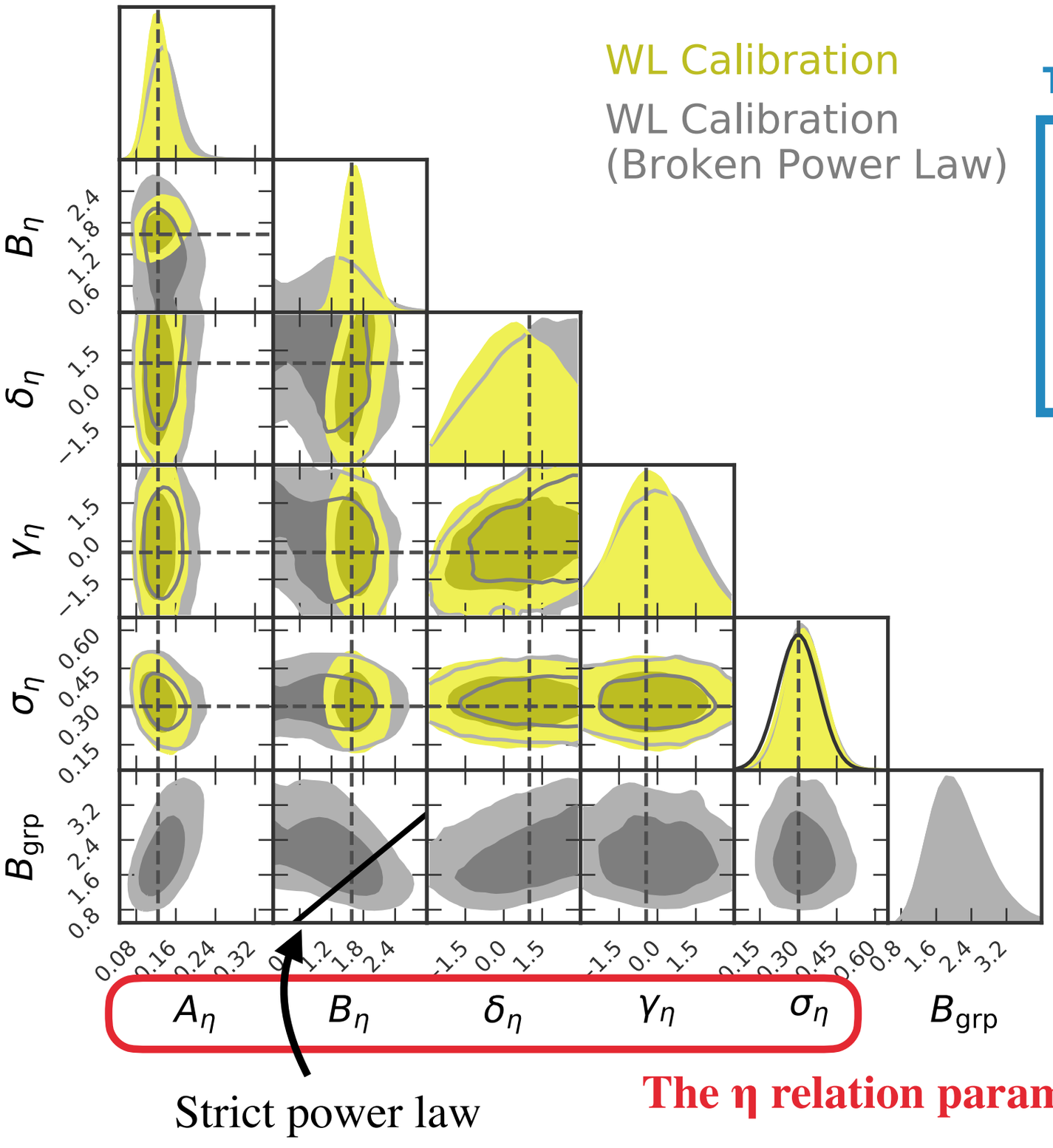






Chiu+22

WL Mass Calibration Alone Modelling



Take-home:

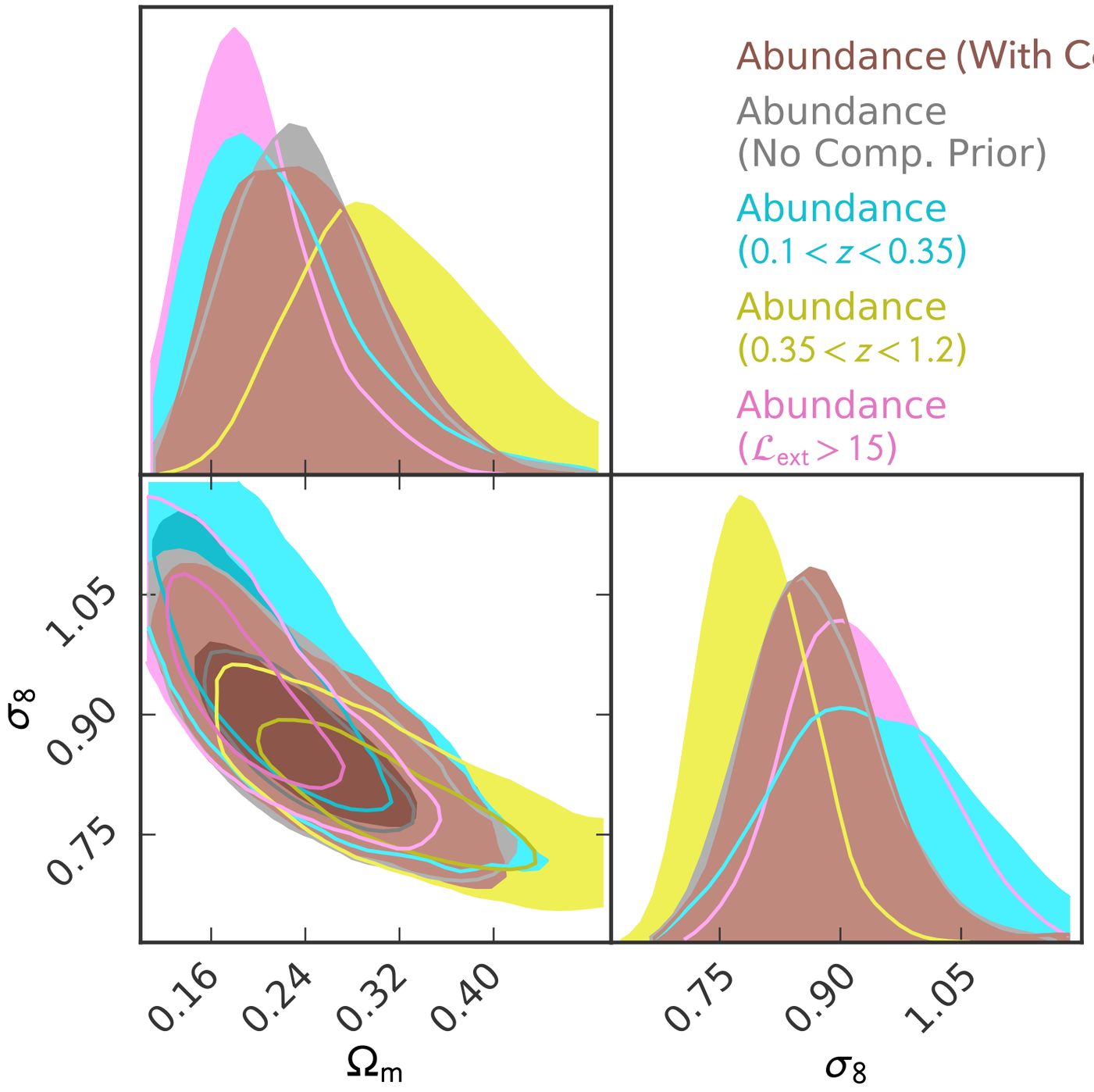
The WL mass calibration does not prefer a broken power law in the η-M relation

The η-M-z relation (strict power law)

$$\langle \ln \eta | M_{500} \rangle = \ln A_\eta + \left[B_\eta + \delta_\eta \ln \left(\frac{1+z}{1+z_{piv}} \right) \right] \times \ln \left(\frac{M_{500}}{M_{piv}} \right) + C_{SS,\eta} \times \ln \left(\frac{E(z)}{E(z_{piv})} \right) + \gamma_\eta \times \ln \left(\frac{1+z}{1+z_{piv}} \right) - 2 \times \ln \left(\frac{D_L(z)}{D_L(z_{piv})} \right) + \ln \left(b_\eta (M_{500}, z) \right)$$

The η relation parameters

Abundance Alone Modelling

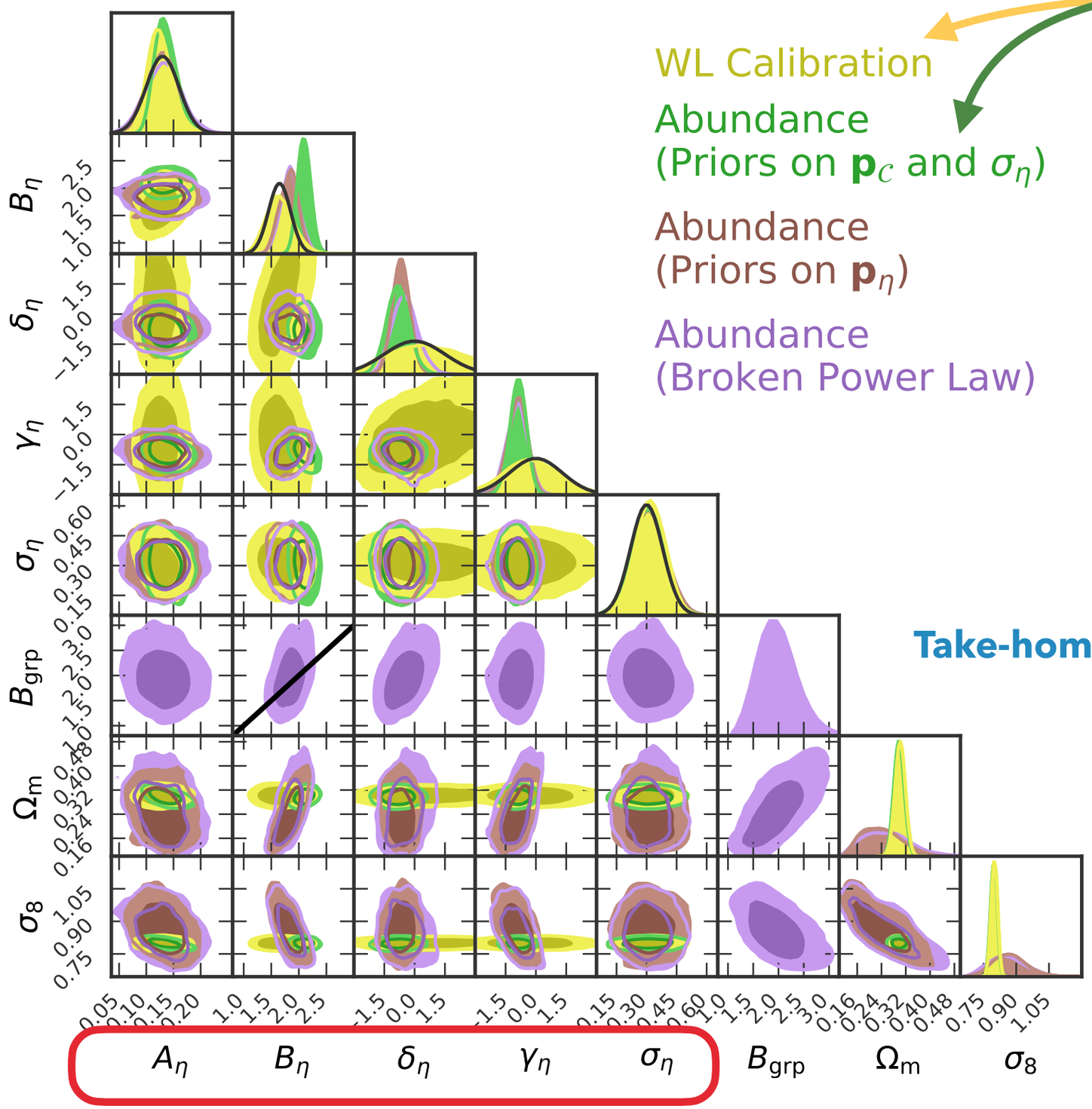


Take-home:

Cosmological constraints from the self-calibrations of subsamples are consistent

(In the self-calibrations, WL-informed priors are applied to the η relation parameters)

Consistency Test on the Count Rate Relation



Fixed cosmology

WL Calibration

Abundance
(Priors on $\mathbf{p}_C$ and σ_η)

Abundance
(Priors on $\mathbf{p}_\eta$)

Abundance
(Broken Power Law)

- Fix cosmological parameters (Ω_m and σ_8) in the self-calibration (green contours)
- The constraints on the η relation parameters are consistent

Take-home:

➡ No strong tensions between the WL mass calibration and the self-calibration

The η relation parameters

The Joint Modelling of Mass Calibration and Abundance

NCKU

WL Calibration

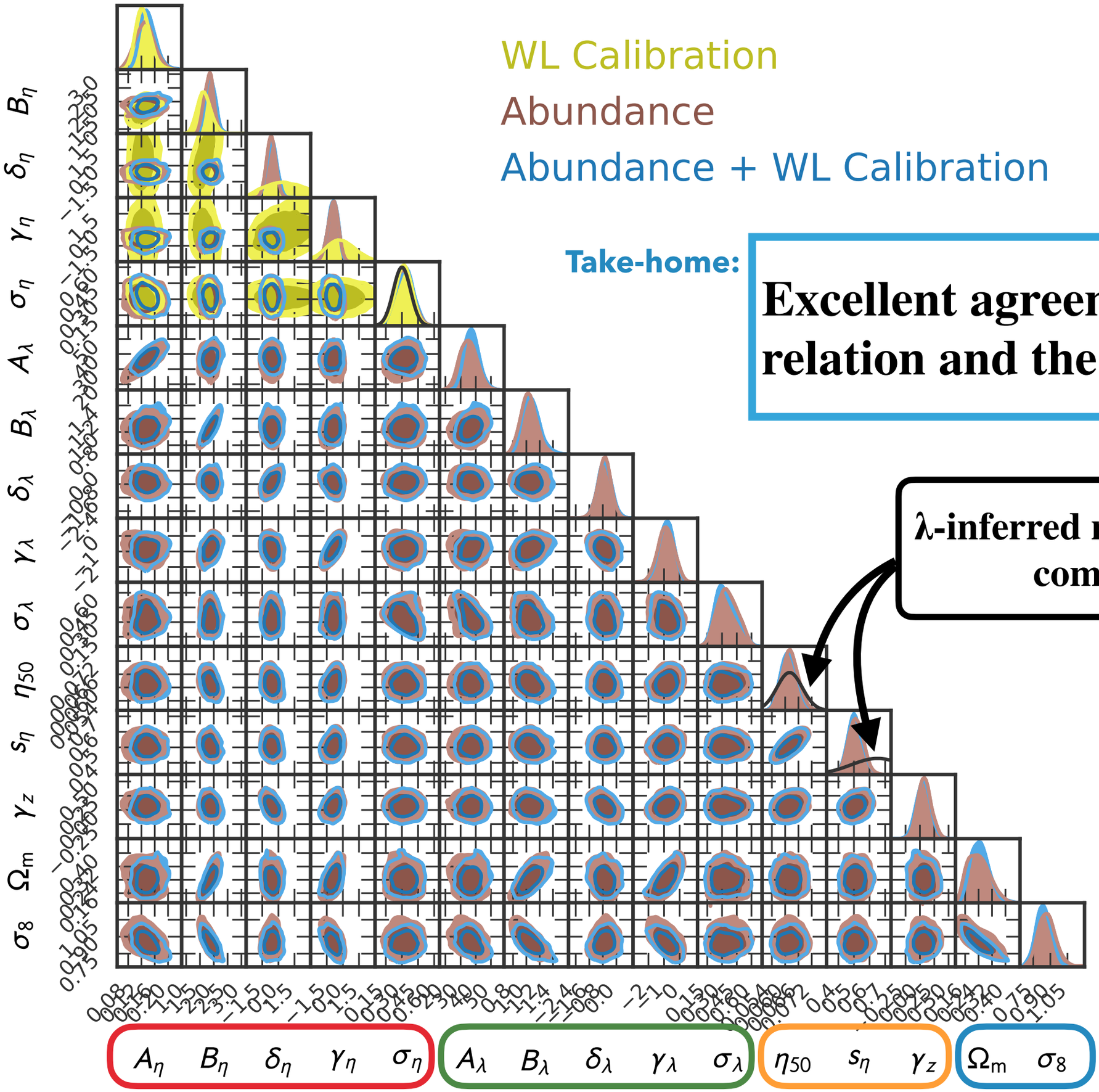
Abundance

Abundance + WL Calibration

Take-home:

Excellent agreements in the rate relation and the completeness!

λ-inferred measurements of completeness



The η relation

The λ relation

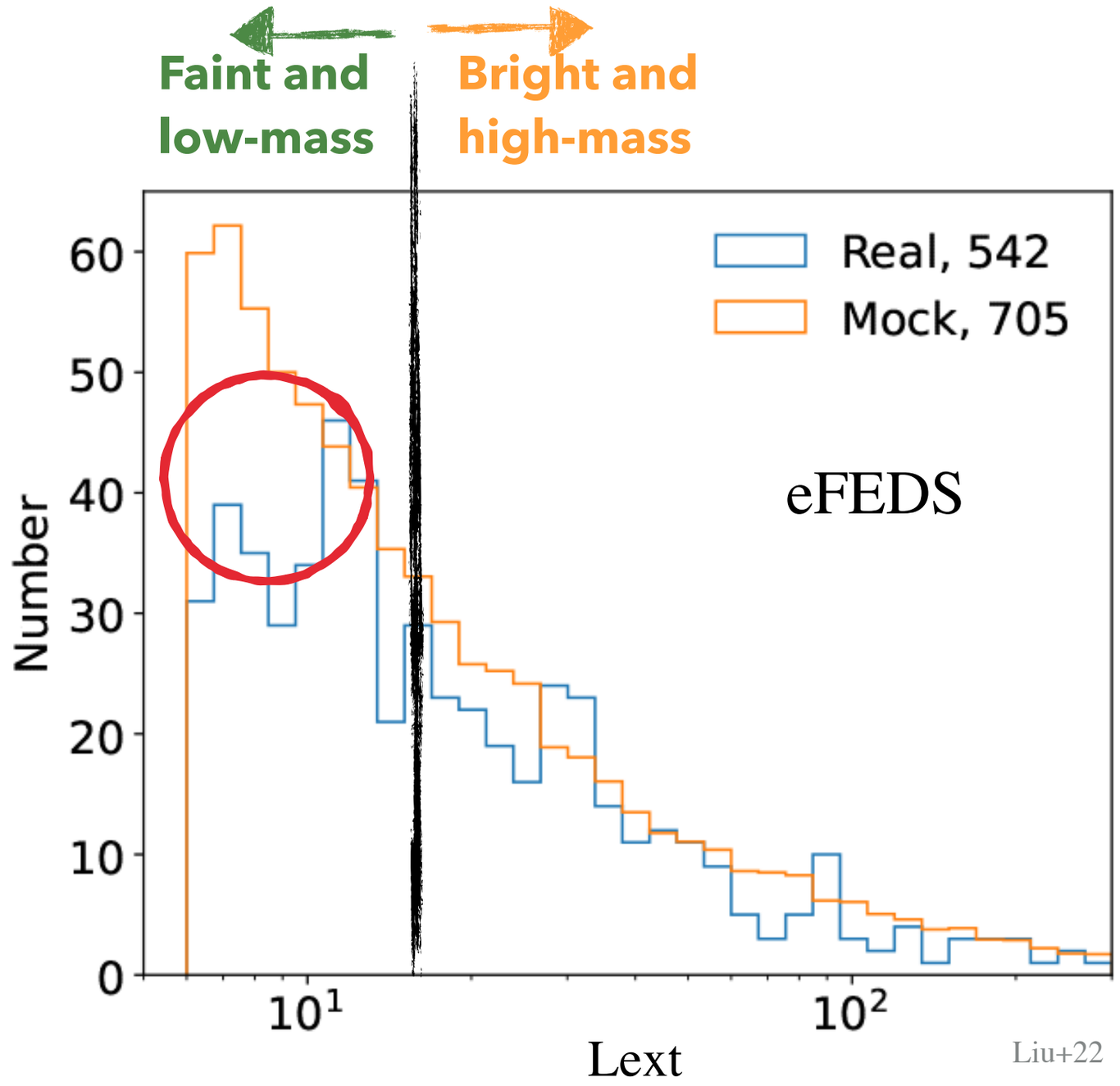
Completeness

Cosmology

The Inconsistency Between the Data and Simulations

A deficit seen in the low L_{ext} end implies incomplete X-ray physics in the sims?

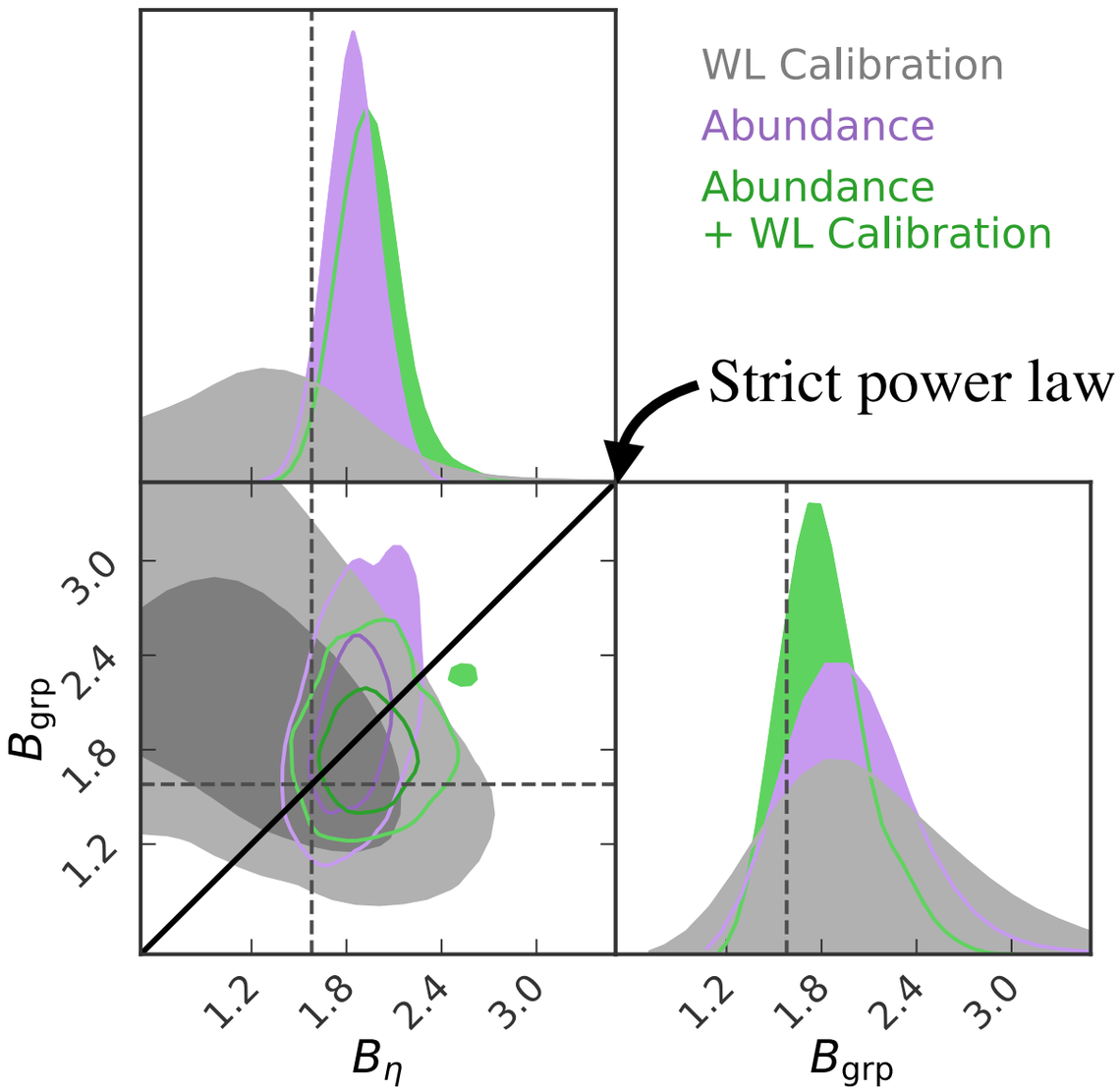
The sim-inferred results might be limited to bright clusters
➡ A much smaller sample

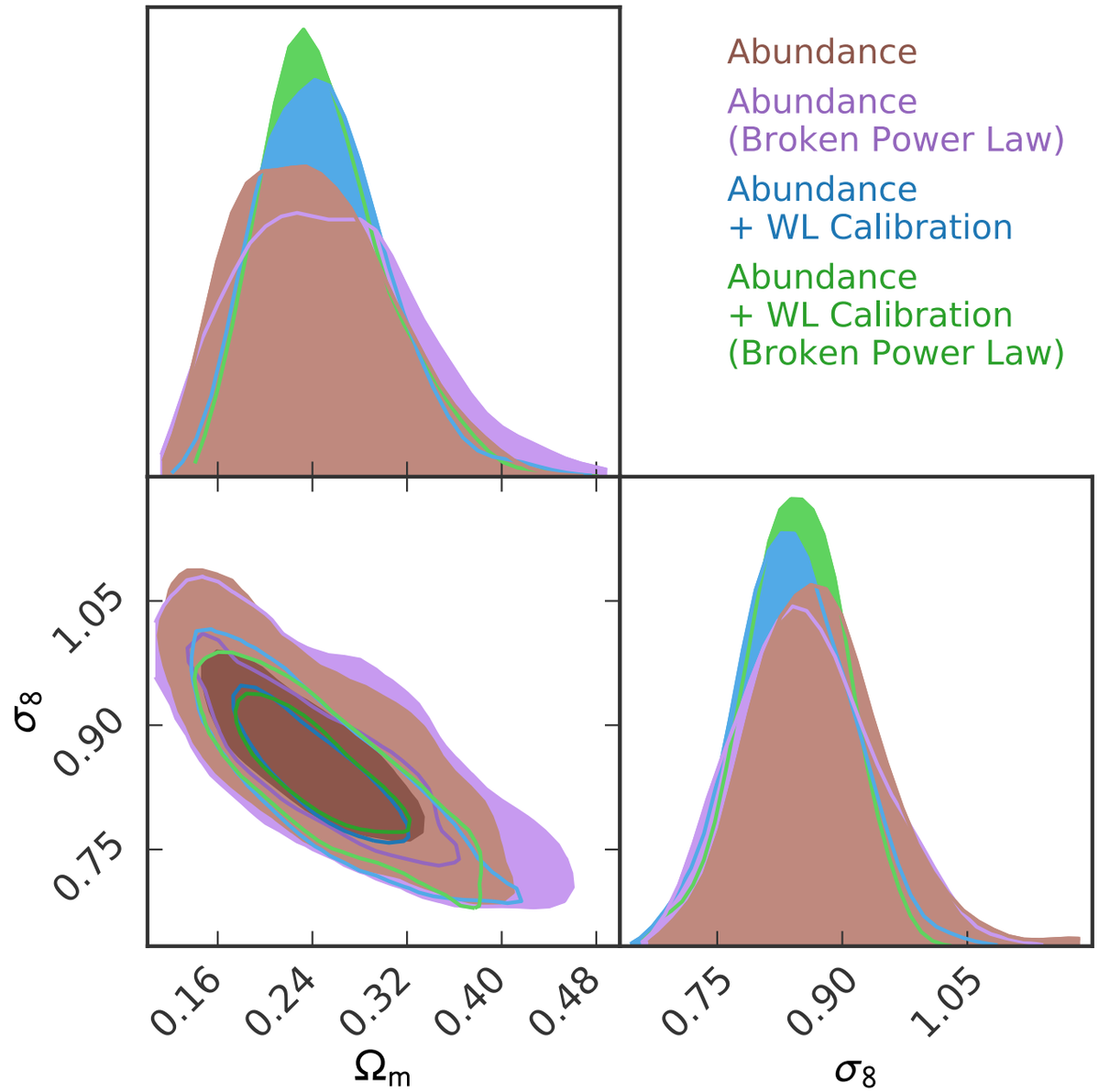


Liu+22

Broken Power Law on Cosmology

With the Broken power law
in the η relation





Take-home:

- **No signs of a broken power law (which cannot explain the deficit at low L_{ext})**
- **Cosmology is not sensitive to the broken power law**

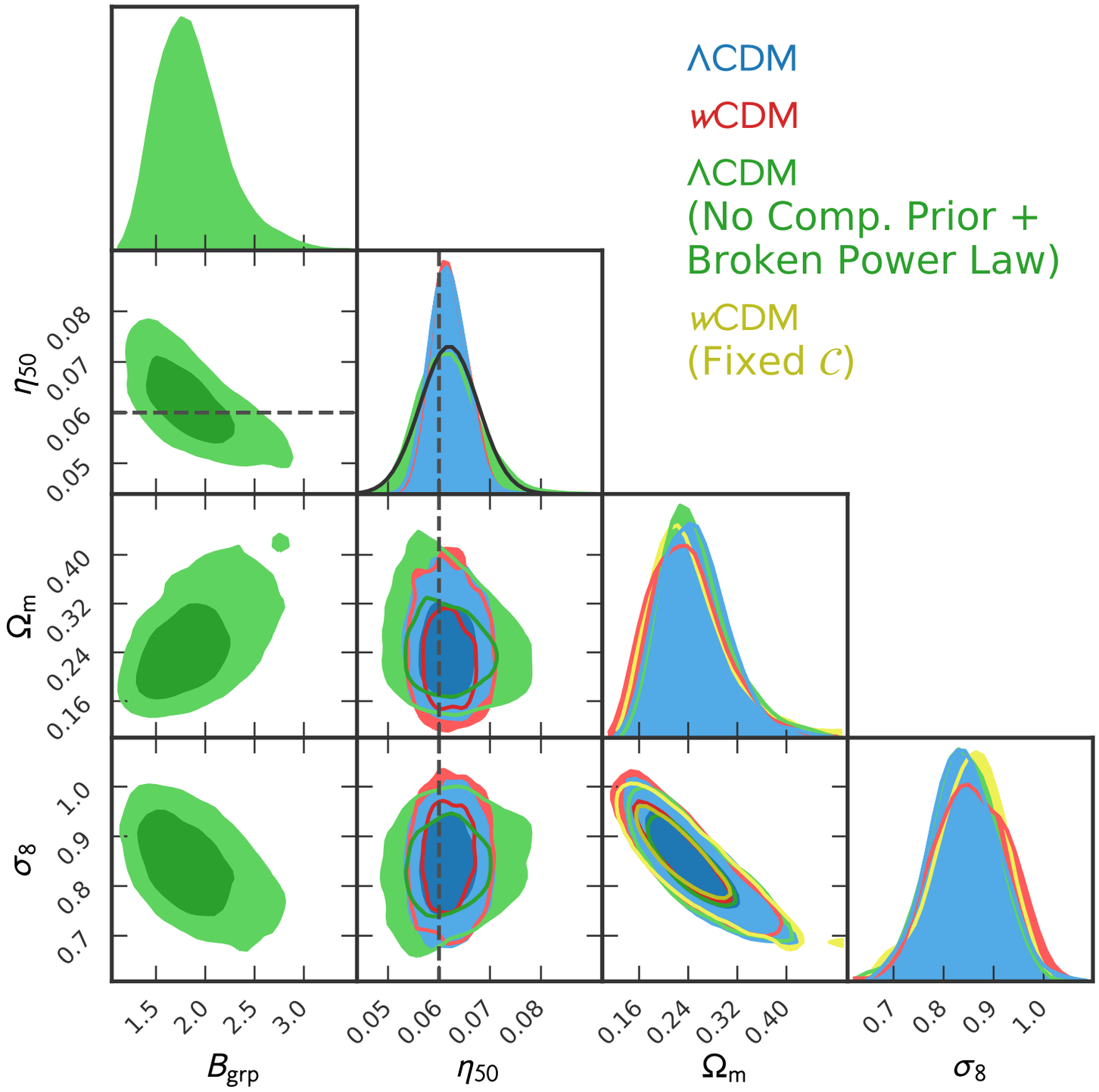
Notes on Completeness and Broken Power Law

NCKU

◉The degeneracy between the completeness and the broken power law of η

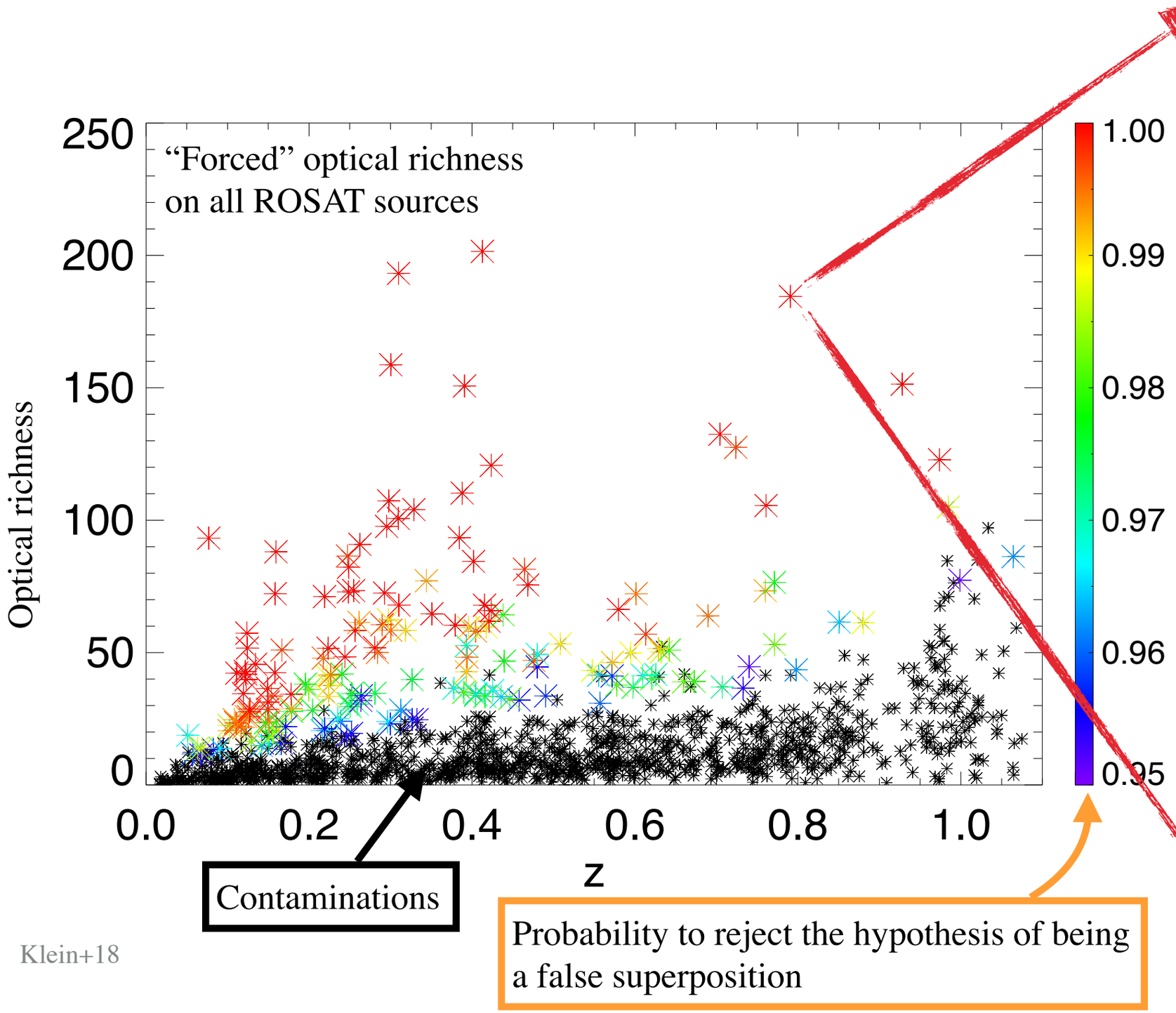
➡ Improve the completeness constraints to probe the population of faint clusters (see also Salvati+22 for SPT x Planck)

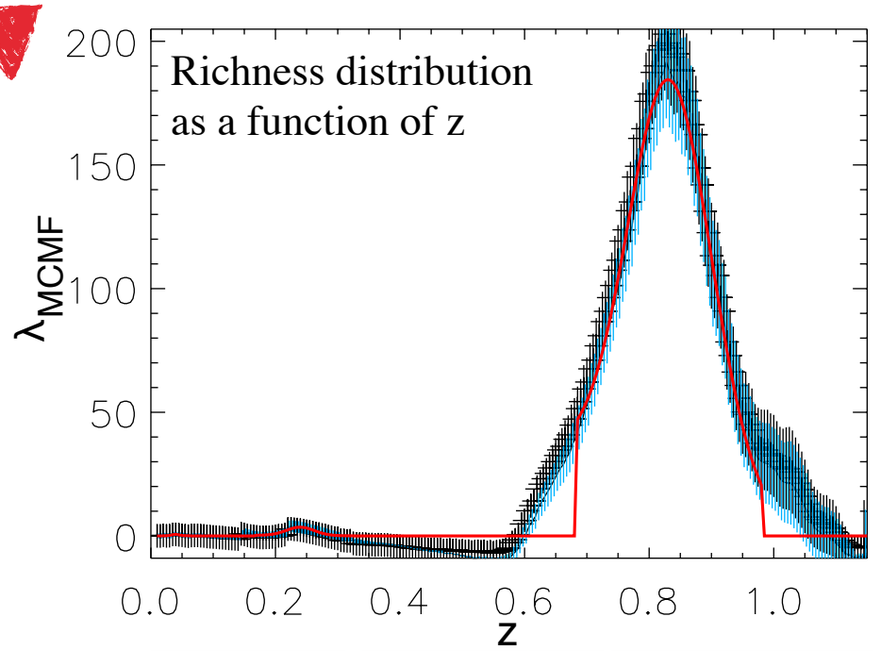
◉Constraints are not sensitive to the precision of the X-ray completeness

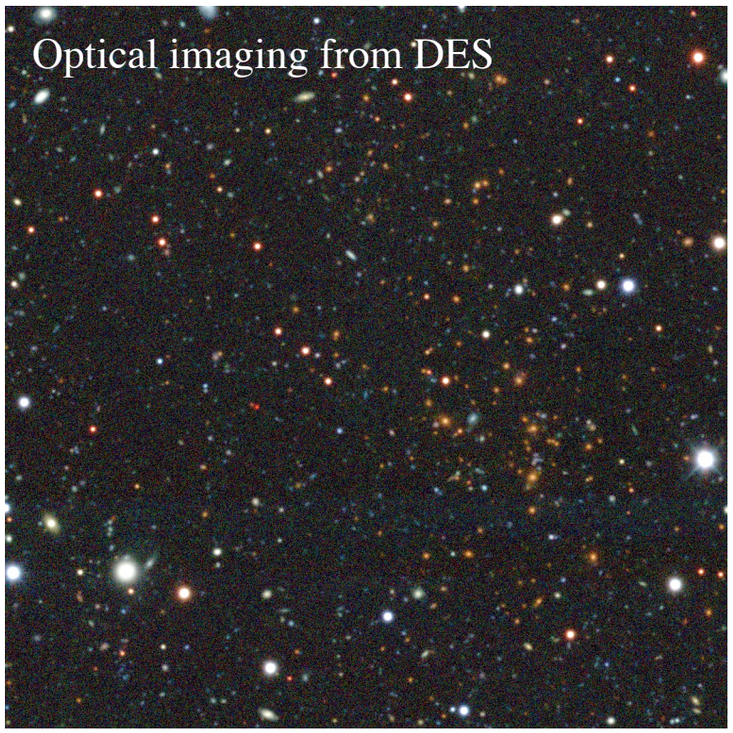


Multi-Component Matched Filter (MCMF) Cluster Confirmation

NCKU







Klein+18

A “z-dependent” cut on richness removes contaminations in an X-ray sample

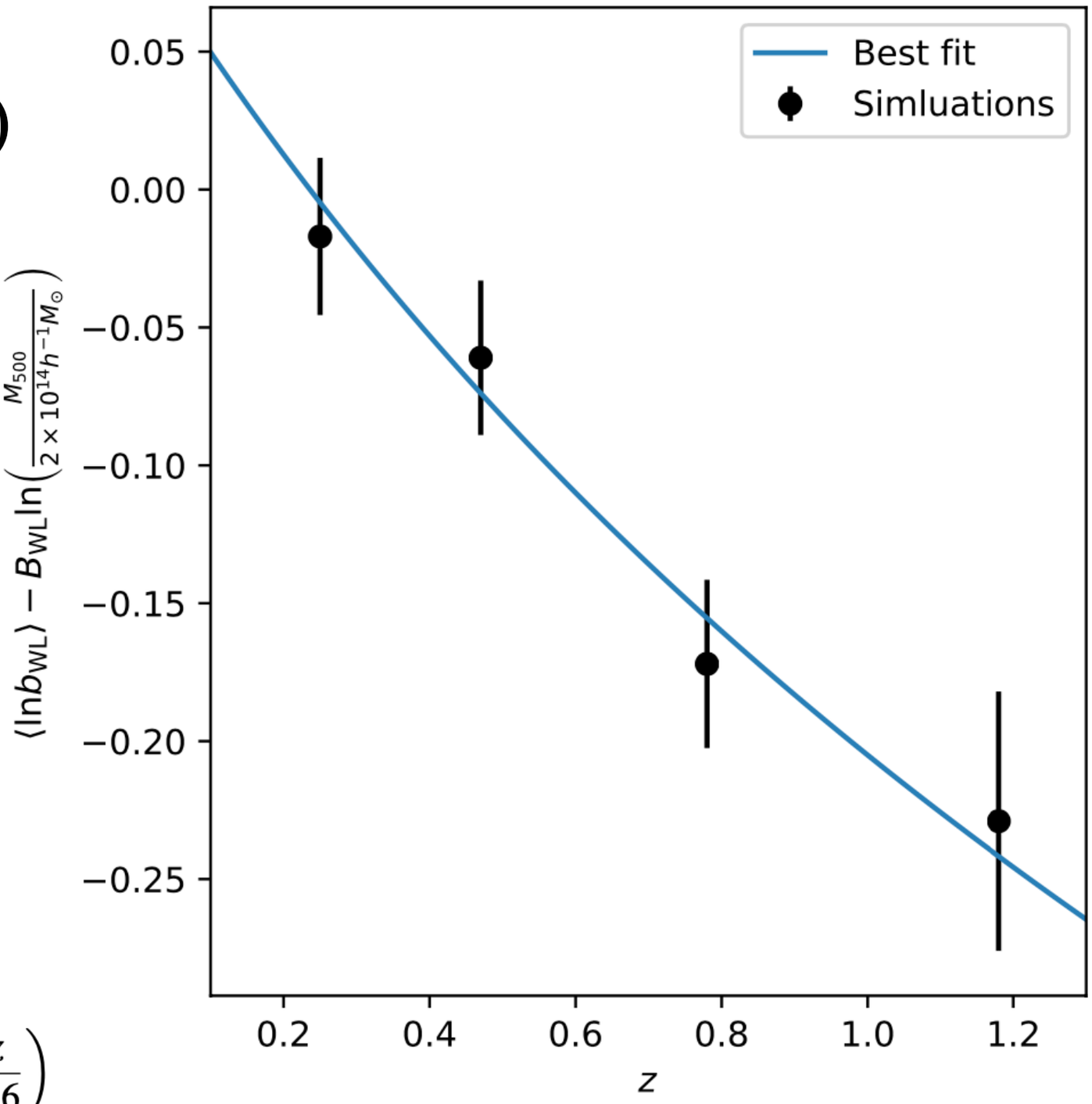
Weak-Lensing Mass Bias


S. Grandis


S. Bocquet

Simulation-based calibrations (Grandis+21)

- Magneticum hydrodynamical simulations (Dolag in prep.)
- Observed weak-lensing properties as inputs
- Weak-lensing mass bias as a function of true mass and redshift



Chiu+22

The M_{wl}–M_{500}–z relation

$$\langle \ln b_{\rm WL}(M_{500}, z) \rangle \equiv \left\langle \ln\left(\frac{M_{\rm WL}}{M_{500}}\right) \right\rangle =$$

$$\ln A_{\rm WL} + B_{\rm WL} \times \ln\left(\frac{M_{500}}{2\times10^{14}h^{-1}{\rm M}_\odot}\right) + \gamma_{\rm WL} \times \ln\left(\frac{1+z}{1+0.6}\right)$$